Anatomy of an enigma: an osteological investigation of the Namibian festive gecko (*Narudasia festiva*: Gekkonidae: Gekkota)

Juan D. Daza,[1,2] Janina Aurich[2,3] and Aaron M. Bauer[2]

[1]CONICET, Instituto de Herpetología, Fundación Miguel Lillo, San Miguel de Tucuman, Tucumán, Argentina; [2]Department of Biology, Villanova University, 800 Lancaster Avenue, Villanova, Pennsylvania 19085, USA; [3]Argelanderstrasse 139, Bonn D-53115, Germany

Abstract

Daza, J.D., Aurich, J. and Bauer, A.M. 2012. Anatomy of an enigma: an osteological investigation of the Namibian festive gecko (*Narudasia festiva*: Gekkonidae: Gekkota). — *Acta Zoologica* (Stockholm) **93**: 465–486.

The monotypic genus *Narudasia* is a poorly studied Namibian endemic gekkonid lizard. It has been hypothesized to have close relationships with a diversity of other gekkotan genera, including representatives of three of the currently recognized families of geckos, but most such interpretations have been based solely on overall morphological similarity. X-ray CT scans, cleared-and-stained specimens and conventional radiographs were used to provide a detailed osteological description of *N. festiva*, with an emphasis on the cranium. *Narudasia* exhibits a number of features associated with miniaturization, including a relatively large neurocranium and a bulging occipital condyle. However, many skeletal features differ from other minaturized taxa but are shared with one or more larger-bodied gecko taxa. *Narudasia* shares a number of putatively derived features with at least some representatives of a large clade of Afro-Malagasy gekkonids, but at present neither molecular nor osteological data adequately resolve its relationships. It remains a phylogenetic enigma, but more extensive osteological taxon sampling across the Gekkota may ultimately reveal synapomorphies uniting *Narudasia* with particular Afro-Malagasy genera.

Juan D. Daza, Department of Biology, Villanova University, 800 Lancaster Avenue, Villanova, Pennsylvania 19085, USA. E-mail: juan.daza@villanova.edu

Introduction

The gekkonid fauna of southern Africa is particularly rich, with approximately 140 species recorded to date. The majority of these occur in the more arid regions in the west of the subcontinent, and Namibia supports a particularly diverse gekkonid fauna (Branch 1988, 1998; Griffin 1998, 2000, 2003; Bauer 1999). Although there are many gecko species endemic to Namibia, mostly in the genus *Pachydactylus* (Bauer *et al.* 2006; Bauer 2010), there is only one endemic gecko genus and indeed, only one strictly endemic reptile genus of any kind, the monotypic festive gecko, *Narudasia*.

Narudasia festiva was described by Methuen and Hewitt (1914), who named the gecko after the farm on which it was found, Narudas, in the Karasberg Mountains of southeastern Namibia (Fig. 1). It ranges across much of southern and central Namibia in areas where suitable rocky substrate is present, from the Hunsberg in the south to Okahandja in the north (Griffin 2002, 2003). *Narudasia* is absent from the dunes and gravel plains of the Namib, but approaches the desert near Swakopmund in central Namibia and in the Lüderitz District to the south, where it occupies areas that provide it with suitable rock crack retreats (FitzSimons 1938; Haacke 1970) (Fig. 2A). Although it occurs only a few tens of metres from the Orange River, which forms the southern border of Namibia, there are no records from adjacent South Africa, despite intensive searches (Bauer and Branch 2003). Narudasia occupies an elevational range from ca. 200 m near the lower Orange River to at least 1300 m at Satansplatz. The species' conservation status has been considered 'secure' (Griffin 2002, 2003). This is supported by its broad distribution (Fig. 1), including several protected areas (e.g. Stuart 1980), and occurrence in areas that are little influenced by
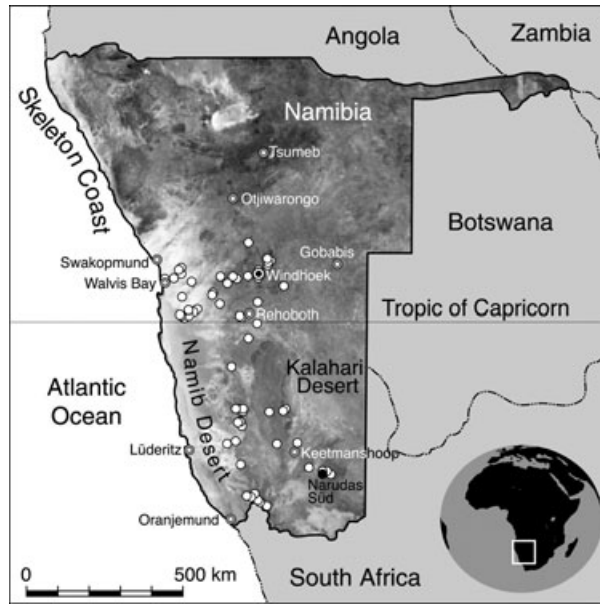
human activity and *N. festiva* is a species of Least Concern under IUCN categorization.

Narudasia is one of the smallest southern African geckos, with a maximum snout-vent length of 32 mm (Visser 1984). The head and body are greatly flattened and the limbs and digits are relatively long (Figs 2B,C and 3). All digits are clawed, and no adhesive pads are borne on the subdigital surfaces. The snout is relatively pointed, the pupils are vertical, and there are no precloacal or femoral pores. The coloration is variable, especially between adults and juveniles (Methuen and Hewitt 1914; Fig. 3), but in dorsal view, the body usually shows a dun coloration, varying from grey purple to chestnut brown with transverse rows of white to cream spots, each bordered anteriorly by dark brown to black markings. Additional white and brown markings are present on the head and limbs. The original tail is olive-yellow to yellow or orange with paired narrow black and white (or pale orange) bands (Fig. 2B), whereas regenerated tails are typically a bright yellow or orange, or a much duller grey to greyish-yellow (see photographs in FitzSimons 1943; Visser 1984; Branch 1988, 1993, 1998; Alexander and Marais 2007; Fig. 2C). The ventral region is dirty white to greyish, with yellow around the cloaca. Detailed descriptions are provided by FitzSimons (1938, 1943) and Loveridge (1947).

The biological literature treating *N. festiva* is limited. The species is typically regarded as diurnally active (Arnold 1990; Röll 2001) or as crepuscular (FitzSimons 1943; Alexander and Marais 2007). Clutch size is two and multiple clutches of small (7.6 × 6 mm) eggs may be laid (FitzSimons 1938, 1943; Branch 1993). FitzSimons (1938, 1943) reported finding eggs in late July, and Visser (1984) found only small
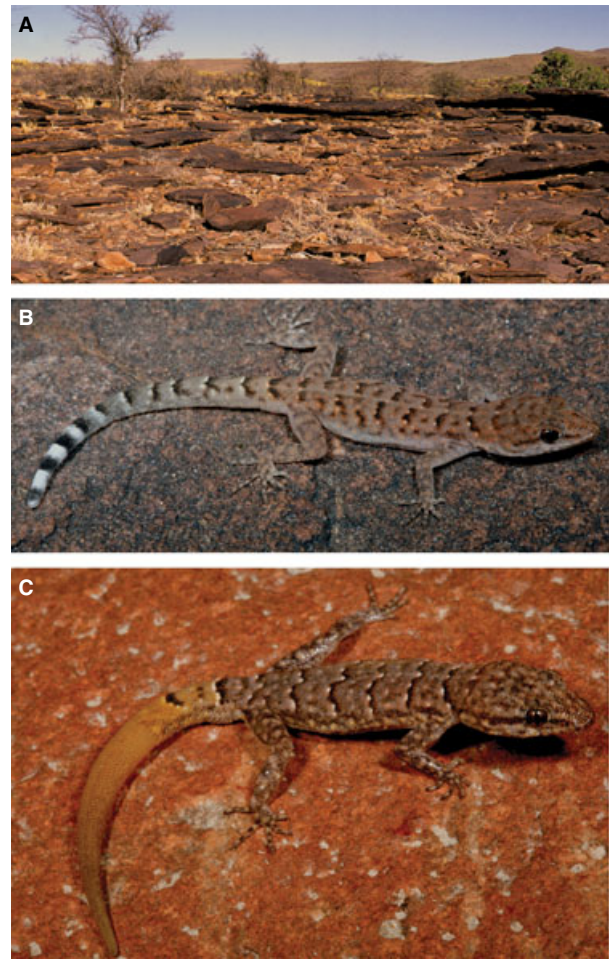

Fig. 2—**A.** typical rocky habitat *of Narudasia festiva* at the type locality on Farm Narudas Süd, Karasburg District, Karas Region, southern Namibia. Specimens from the same locality, showing — **B.** original and — **C.** regenerated tails. Specimen pictures courtesy of Johan Marais.

oviductal eggs in April and suggested that clutches were laid in summer. Diet has been reported to include ants, flies and other small insects (FitzSimons 1943). Lawrence (1936) indicated that he found no mites on the *Narudasia* he examined, but Visser (1984; fig. p. 65, top) illustrated them on the ventral surface of a specimen, and they are commonly encountered on wild-caught specimens (AMB personal observation).

Despite its relative obscurity, *Narudasia* has been the object a disproportionate amount of speculation with respect to its phylogenetic placement. Methuen and Hewitt (1914) believed that it was similar to *Stenodactylus* (a North African and Arabian genus) and *Homonota* (a southern South American genus) but could be differentiated by the condition of the ventral scales of the digits. Parker (1936) found it nearly indistinguishable from *Gymnodactylus*, which then included taxa now distributed among a number of chiefly Asian genera, as well as the South American *Gymnodactylus* sensu stricto.
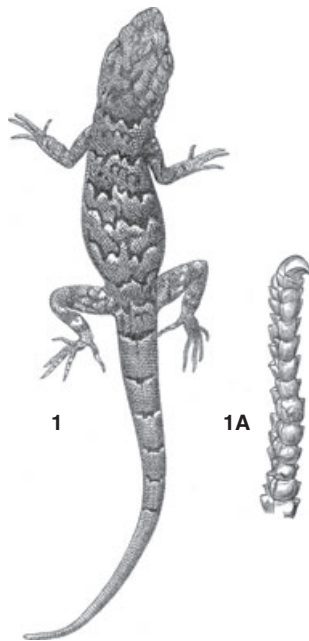
Fig. 3—Reproduction of the illustrations from the original description of *Narudasia festiva*. Methuen and Hewitt (1914), plate XIV). 1. Dorsal view of whole specimen, 1a. ventral view of (presumably 4th) toe showing the exposed claw and the lamellae.

Loveridge (1947) synonymized it with the Moroccan genus *Quedenfeldtia*. This generic allocation was followed by Mertens (1955), although he noted its similarity to *Tropiocolotes*, a North African and Near Eastern genus and subsequently (Mertens 1971) rejected Loveridge's (1947) action. Haacke (1976) proposed a possible relationship with *Ptenopus* on the basis of geography and digital structure. Underwood (1954) and Kluge (1967, 1987) included it within the Gekkoninae, but without any specific suggestions of relationship, and Bauer (1990a) and Haacke (1997) noted that the placement of *Narudasia* within the phylogeny of African gekkonids was uncertain. Kluge (1995), however, used *Narudasia* together with *Cnemaspis*, *Saurodactylus* and *Quedenfeldtia* as an outgroup in a study dealing with sphaerodactyl geckos. Its inclusion in this study was based on *Narudasia*'s shared lack of cloacal bones and sacs with these New World geckos (Kluge 1982; Arnold 1990, 1993; Kluge and Nussbaum 1995). Russell and Bauer (2002) highlighted *Narudasia* as one of a number of problematic gekkonid taxa, whose relationships had not been clarified by the accumulation of data through the latter half of the 20th century. Molecular phylogenetic analyses have likewise been inconclusive with respect to the affinities of *Narudasia*, except to confirm its placement in the Gekkonidae (sensu Gamble *et al.* 2008a) and to demonstrate that it is deeply divergent from all other genera. Molecular phylogenetic analyses based on restricted subsets of taxa have recovered *Narudasia* with possible affinities to the South Asian *Calodactylodes* (Feng *et al.* 2007) or to Afro-Malagasy genera in

general (Han *et al.* 2004; Gamble *et al.* 2008a,b), but without strong support. Recent skeletal examinations have suggested some similarities to the geographically proximate but genetically highly divergent *Rhoptropus* (Daza 2008).

Even a multi-gene analysis of all gekkotan genera and more than 700 species (Bauer *et al.*, unpublished data) does not clarify the relationships of *Narudasia*, which, along with another southern African genus, *Ptenopus*, and several Indian Ocean taxa, remain among the most enigmatic of all gekkotan groups (Russell and Bauer 2002). Given this difficulty, we here provide a detailed osteological description of *Narudasia festiva* that may serve as the basis for the identification of characters of possible phylogenetic value.

Materials and Methods

Specimens of *Narudasia festiva* were examined from museum collections in southern Africa, North America and Europe and all unique localities were plotted (Fig. 1) to assess the species' distribution. Institutional abbreviations are as follows: AMB, Aaron M. Bauer personal collection, Villanova University, Villanova, USA; AMG, Albany Museum, Grahamstown, South Africa (now incorporated into Bayworld [PEM]); BMNH, The Natural History Museum, London, UK; CAS, California Academy of Sciences (CAS), San Francisco, CA, USA; FMNH, Field Museum of Natural History, Chicago, IL, USA; MCZ, Museum of Comparative Zoology, Harvard University, Cambridge, MA, USA; NMN, National Museum of Namibia, Windhoek, Namibia (formerly State Museum Windhoek); PEM, Bayworld (formerly Port Elizabeth Museum), Port Elizabeth, South Africa; SAM, South African Museum, Cape Town, South Africa; SMF, Forschungsinstitut Senckenberg, Frankfurt, Germany; TM, Ditsong: National Museum of Natural History (formerly Transvaal Museum), Pretoria, South Africa; USNM, National Museum of Natural History, Washington, DC, USA; YPM, Yale University Peabody Museum, New Heaven, CT, USA; ZFMK, Zoologisches Forschungsmuseum Alexander Koenig, Bonn, Germany. Additional comparative material was examined from the collections of the American Museum of Natural History, New York, NY, USA (AMNH), the Fundación Miguel Lillo, Tucumán, Argentina (FML) and the Institute of Paleontlogy, Polish Academy of Sciences, Warsaw, Poland (ZPAL).

For osteological description, it is desirable to use as many techniques as possible, including histological sections and X-ray microtomography, because each provides information that overlaps or complements the others. Traditional radiography is convenient because it is non-destructive, images are revealed instantaneously (using a digital detector), and many specimens can be examined quickly, cheaply and easily. Nonetheless, the overlap of structures limits visualization and makes some structures hard to interpret. This kind of preparation is mainly useful for obtaining meristic and morphometric data. High-resolution X-ray computed tomography is a much

superior method, but is costly and thus limits the number of specimens that can be prepared. Cleared-and-stained preparations are inexpensive and provide information about cartilage and the state of ossification of bones, but it is destructive of soft tissues, not suitable for rare species, and cannot be used very effectively on non-formalin-fixed material (Bauer 1986).

For clearing and staining, we followed the protocol of Bauer (1986), reducing time in most solutions to compensate for the small size of *Narudasia*. Specimens were fixed in 10% neutral buffered formalin, skinned and eviscerated, and washed in two changes of distilled water for 2 h each. Cartilage was stained for 24 h in a solution of 20 mg alcian blue 8GX, 70 mL 100% ethanol and 30 mL glacial acetic acid after which the specimens were transferred through two changes of 100% ethanol for 6 h each and through a graded ethanol series (95%, 75%, 40%, 15%, distilled water – 1 h in each step). Partial maceration was carried out in a solution of 30 mL saturated aqueous sodium borate, 70 mL distilled water and one gram trypsin at 38 °C until the body became limp and the skeleton visible (approximately 6 h). Bones were stained for 1 h in 0.5% potassium hydroxide solution containing alizarin red S powder saturated in 70% ethanol then transferred through a graded solution of 0.5% KOH and glycerine (3 : 1, 1 : 1, 1 : 3). A small amount of hydrogen peroxide was added in the first two steps to depigment the tissue. Specimens were left in each step for several days and transferred to glycerine for storage when the body tissues were transparent.

Specimens were X-rayed using Polaroid Type 55 (positive/negative) film in a Faxitron closed cabinet X-ray unit at a voltage of 20 kVb for 20 s. Negatives were scanned and edited in Adobe Photoshop® to optimize contrast and facilitate examination of fine structures.

The head of a whole preserved *Narudasia festiva* (CAS 186278) was scanned at the High-Resolution X-ray CT (HRXCT) Facility at The University of Texas at Austin with a FeinFocus microfocal X-ray source operating at 180 kV and 0.13 mA. The field of reconstruction was of 6.5 mm with interslice spacing of 0.01602 mm for the original scan, and one pixel equals 0.0063 mm for horizontal and sagittal reslicings. Each slice image was gathered at 1024×1024 pixel resolution as a 16-bit TIFF image. Three-dimensional rotations and sections along the three orthogonal axes were generated from the original slices.

Results

Overall description of the skull and jaw

The skull of *Narudasia festiva* is almost oval in dorsal view. It is very flat, even for geckos, which typically have depressed skulls (Kluge 1962, 1967). It is longer than wide, with its widest point at the level of the quadrates (q, Fig. 4A). The anterorbital portion of the snout and the orbit each account for approximately 30% of the total skull length. The posterolateral extension of the frontoparietal suture is located at 63% of

the total skull length, resulting in a very elongate muzzle unit (Frazzetta 1962). The skull table is flat and does not lie at the same level as the supraoccipital. The CT-scanned specimen shows areas of incomplete ossification in the skull, especially at the anterior edge of the parietals where a wide parietal fontanelle is visible (par, Fig. 4A), whereas in the cleared-and-stained specimens, this area is completely closed. The supraoccipital is exposed, as in other miniaturized gekkotans (e.g. sphaerodactylids, *Homonota, Aprasia*).

In the ventral view (Fig. 4B), the skull exhibits an oval suborbital fenestra, which is slightly reduced by an extensive, transverse open contact suture between the palatine and the pterygoid. This condition, together with reduced contact between the palatine and the vomer, results in a highly mobile palate. The palate displays the paleochoanate condition (Lakjer 1927; Rieppel *et al.* 2008), with the fenestra vomeronasalis and choana in a continuous slit. The choanal canal of the palatine is short and shallow. The premaxillary-vomerine fenestra is absent because of extensive medial contact of the maxillary lappets. The interpterygoid vacuity is wide and extends anteriorly without invading the medial contact of the paired vomers.

In the lateral view (Fig. 4C), the skull is pointed and wedge shaped, with a gradual inclination of the snout. The rostrum anterior to the external nares is very short, having an anterior extension of about three tooth loci. The tip of the snout is formed exclusively by the premaxilla. The skull is very open, with the eye socket and the temporal fenestrae combined in a single space as a consequence of the loss of the postorbital bar and the supra- and infratemporal arches, a widespread condition among Gekkota. Ten per cent of the total eye diameter extends above the dorsal edge of the frontal bone, resulting in somewhat bulging eyes.

The premaxillary–maxillary arcade forms a complete overbite of the jaw (Fig. 4B,C). The mandibular unit is flat ventrally and presents its highest point at the level of the coronoid. The jaw is almost straight posteriorly but gradually curves anteriorly in the dentary section (Fig. 4C).

Dermatocranium

The premaxilla (pmx, Fig. 4A,C,D) is unpaired, with 12 tooth loci. It forms the tip of the snout, curving latero-posteriorly to contact the maxilla. The teeth are pleurodont and isodont; in CAS 186278, eight teeth are fully functional and four are missing or in a stage of replacement. The premaxilla consists of the anterior portion of the dental arcade and the ascending nasal process (asnp, Fig. 4A). In the dorsal view, the former part is kidney shaped and contacts the maxilla posterodorsally in an overlapping suture. The premaxillary shelf is horizontal in profile, and an incisive foramen is absent. The ascending nasal process is a thin, elongate, bar-like structure that extends dorsally to overlap the nasal bones for about one half of their entire length. The anterior part of the shaft is thicker and corresponds to the narrowest plane of the process;
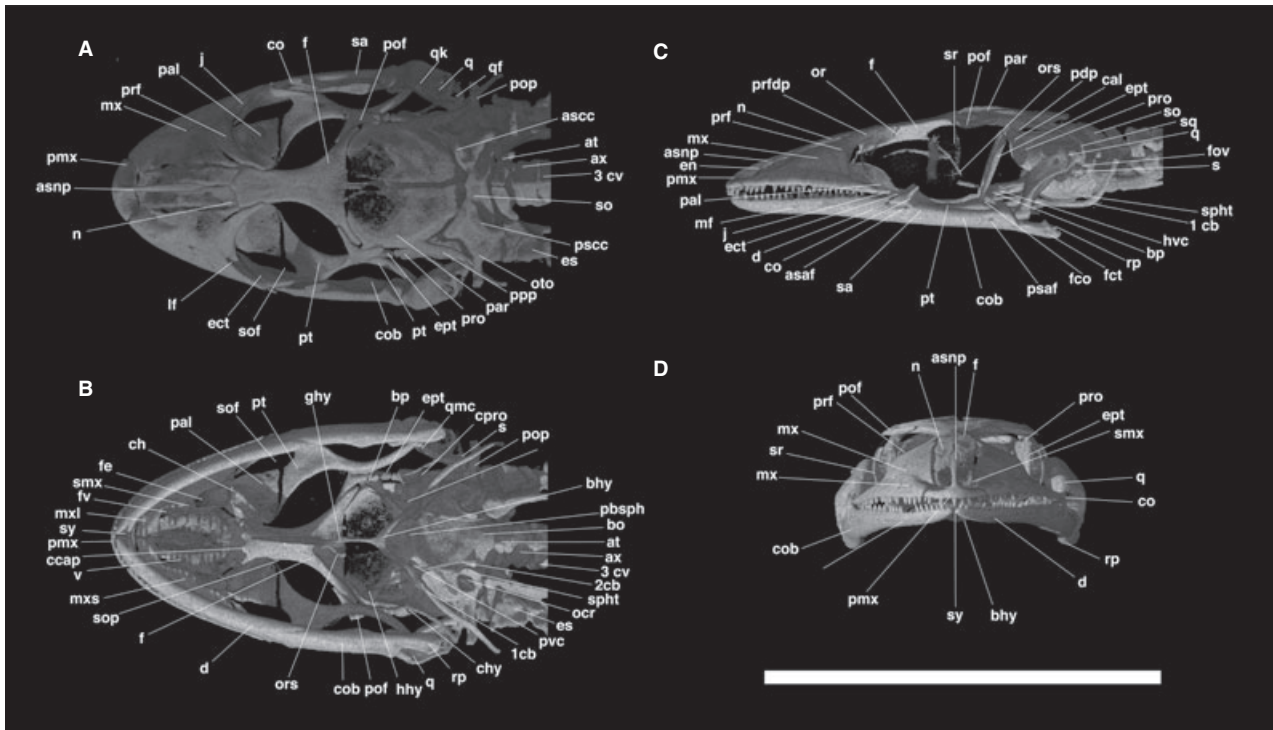
Fig. 4—Skull of *Narudasia festiva* (California Academy of Sciences 186278) in — **A**. dorsal, — **B**. ventral, — **C**. lateral and — **D.** frontal views. Scale bar equals 10 mm. Abbreviations: 1 cb, first ceratobranchial; 2 cb, second ceratobranchial; 3 cv, third cervical vertebra; asaf, anterior surangular foramen; ascc, anterior semicircular canal; asnp, ascending nasal process; at, atlas; ax, axis; bh, basihyal; bo, basioccipital; bp, basipterygoid process; bhy, basihyal; bp, basipterygoid process; cal, crista alaris; ccap, crista cranii anterior process; ch, choana; chy, ceratohyal; cob, compound bone; co, coronoid; d, dentary; ect, ectopterygoid; en, external nares; ept, epipterygoid; es, endolymphatic sac; f, frontal; fe, fenestra exochoanalis; fco, fossa columellae; fct, foramen for the chorda tympani; fov, fenestra ovalis; fv, fenestra vomeronasalis; ghy, glossohyal process; hhy, hypohyal; hvc, groove for course of lateral head vein; j, jugal; lf, lacrimal foramen; mf, mental foramina; mx, maxilla; mxl, maxillary lappet; mxs, maxillary shelf; n, nasal; ocr, occipital recess; oto, otooccipital; or, orbital ridge; ors, orbitosphenoid; pal, palatine; par, parietal; pbsph, parabasisphenoid; pdp, decensus parietalis process; pmx, premaxilla; pof, postorbitofrontal; pop, paroccipital process; ppp, postparietal process; prf, prefrontal; prfdp, dorsal process of prefrontal; pro, prootic; psaf, posterior surangular foramen; pscc, posterior semicircular canal; pt, pterygoid; pvc, posterior opening of vidian canal; q quadrate; qf quadrate foramen; qk; quadrate keel; qmc, quadrate medial column; rp, retroarticular process; s, stapes; sa, surangular; smx, septomaxilla; so, supraoccipital; sof, suborbital fenestra; sop, subolfactory process; spht, sphenooccipital tubercle; sq, squamosal; sc, sclerotic ring; sy, madibular symphysis; v, vomer. Scale bar equals 10 mm.

posteriorly, this process is flattened and abruptly converges into a sharp pointed terminus (Fig. 4A).

The paired maxillae (mx, Figs 4A,C,D and 5) are the largest bones of the snout. These bones have a tall triangular facial process (mxfp, Fig. 5A) located anteriorly, with extensive laminar contact with the nasal, an extensive overlap with the prefrontal, and a slight overlap with the frontal. The facial process has a longitudinal crease that produces a flattened rostral surface that is continued onto the nasal bones. The facial process forms the posterolateral corner of the external naris. Postnarially, this dorsal process bends medially to form a small and almost horizontal depression (mxd, Fig. 5A). The posterior extent of the facial process separates the nasal from the prefrontal. The maxilla contains the superior alveolar canal for the maxillary branch of cranial nerve V and its accompanying blood vessels (Evans 2008; Evans and Manabe

2008). The opening of the superior alveolar canal (sac, Fig. 5B), through which the terminal branches of the maxillary artery and the maxillary branch of cranial nerve V exit to the nasal capsule (Oelrich 1956), lies in the external narial vestibule, at the base of the maxillary lappet (mxlp, Fig. 5B). Near its labial edge, four small foramina pierce the maxilla, the three anteriormost open anteriorly and the most posterior one laterally; these are the passages for the cutaneous branches of the maxillary division of cranial nerve V and the maxillary artery (fmx5, Fig. 5). Dorsal to the 3rd maxillary foramen, at the beginning of the overlapping suture between the maxilla and the prefrontal, there is a larger foramen, than for the cutaneous branch of the lateral ethmoidal nerve (feth, Fig. 5; Oelrich 1956).

The maxillary lappet meets its fellow medially and forms a broad bridge (Häupl 1980) that contacts the vomer
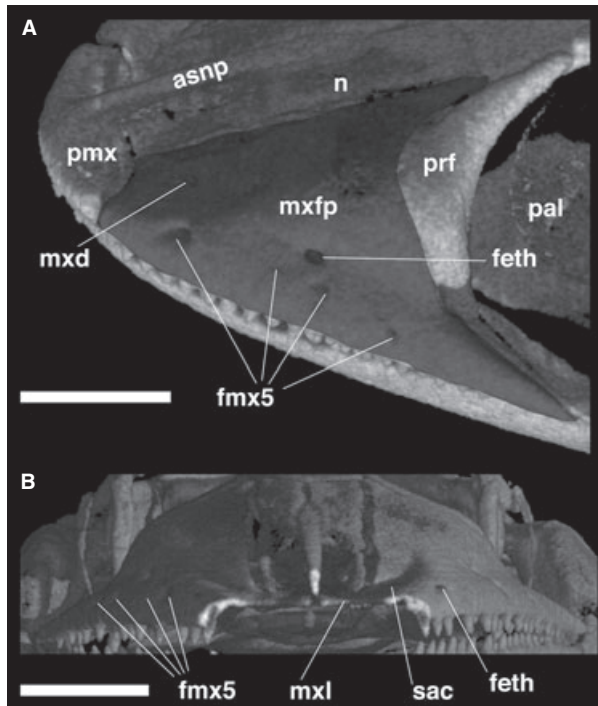
Fig. 5—*Narudasia festiva* (California Academy of Sciences 186278) snout in dorsolateral view — **A**. and coronal slice at the level of the premaxilla-maxilla ventral suture —**B**. Abbreviations: asnp, ascending nasal process; feth, foramen for cutaneous branch of lateral ethmoidal nerve; fmx5, foramina for cutaneous branches of maxillary division of cranial nerve V and maxillary artery; mxd, anterodorsal depression of maxilla; mxl, maxillary lappet; pal, palatine; prf, prefrontal; pmx, premaxilla, mxfp, facial process of maxilla; n, nasal; sac, opening of superior alveolar canal. Scale bar equals 1 mm.

posteriorly and the septomaxilla posterodorsally, separating the premaxilla from the vomer (Kluge 1995; Kluge and Nussbaum 1995; Evans 2008) and excluding it from the fenestra exochoanalis. Posteriorly, the orbital process forms the lateral edge of the lacrymal foramen and is overlapped by the jugal bone. The alveolar border bears 22 tooth loci (20 functional teeth) and extend medially to form a broad palatal shelf (Evans 2008) which bounds the fenestra exochoanalis laterally (Rieppel *et al.* 2008) without contacting or overlapping the vomer.

The nasal (n, Fig. 4A,C,D) is a paired rectangular bone, the anterior half of which is overlapped dorsomedially by the ascending nasal process of the premaxilla, reducing internasal contact to less than one half the length of these elements (n, Figs 4A and 5). Because of this overlap, the medial edges of the nasals bend downwards, forming a concavity. The anterior edge of the nasal is thin and the nasofrontal suture overlaps the anterior portion of the frontal like an inverted 'V'. The ventral surface of the nasals is in contact with the septomaxilla.

The prefrontal (prf, Fig. 4A,C,D) is a triangular circumorbital bone. The anterior portion is extensively overlapped by

the maxilla, leaving exposed only a semilunate lateral surface. The posterior part curves inward forming the orbitonasal flange, which constitutes the posterior wall of the nasal capsule and, together with the palatine, borders a slit-like orbitonasal fenestra. The orbitonasal flange has a vertical ridge extending from the facial surface to the inside of the eye socket. The posterodorsal process (prfdp, Fig. 4C) tapers gradually into a rod-like structure with a rounded point. This process is recessed into the lateral surface of the frontal. Posteroventrally, the prefrontal has a short process that sometimes contacts the jugal and forms the dorsomedial border of the lacrimal foramen.

The frontal (f, Fig. 4) is unpaired, and in the majority of geckos participates with the circumorbital bones in the orbital margin (Daza and Bauer 2010). Its narrowest part is located in the middle at the constriction between the orbits. The length of the observable part of the bone, from the median process to the posterior edge, is approximately as wide as the posterior width. This bone is overlapped anteriorly by the nasals and has narrow anterolateral contact with the maxilla, preventing the nasal from contacting the prefrontal. The posterolateral processes are strut-like and rounded at the end. These processes rest, to a certain extent, on a depression present in the anterolateral corner of the parietal, creating a hinge-like articulation. This articulation has been described in geckos as a syndesmosis, where fibrous tissue rather than cartilage is present on the articulating surfaces (Payne *et al.* 2011). The frontal bone along with the parietal forms a U-shaped, anteriorly arched frontoparietal suture that is highly mobile mesokinetic joint (Versluys 1912; Frazzetta 1962; Iordansky 1966; Rieppel 1984a; Johnston 2010).

The subolfactory processes, which are formed by the crista cranii, are completely fused ventrally, forming a funnel-like structure almost four times as wide anteriorly as posteriorly, which encases the olfactory tracts. There are two sinuses running parallel on the lateral crests of the frontal. The crista cranii possess two peg-like anterior processes that are capped by cartilage.

The postorbitofrontal (pof, Fig. 4A–D) is the posterodorsal circumorbital element and in dorsal view is L-shaped. It clasps the frontal and parietal and its lateral vertex is located anterior to the frontoparietal suture. Its external margins form an almost right angle, while the internal border defines a slightly greater angle. The posterior process is twice the width of the anterior process; both processes terminate in a rounded point. The lateral process extends horizontally and does not curve downwards.

The jugal (j, Fig. 4A) is ventral circumorbital bone; it is reduced to a splint with a thicker anterior part. It has mostly lateral contact with the maxilla and is bound tightly between the maxilla and the ectopterygoid. The jugal contributes narrowly to the rim of the lacrimal foramen, but does not contact the prefrontal.

The parietal (par, Fig. 4A,C) is paired and may be poorly ossified in *Narudasia*, as mentioned earlier. It contacts the

frontal and the postorbitofrontal anteriorly and the squamosal posterolaterally. The parietal and the supraoccipital do not lie in the same plane, and there is a narrow space between them. This lack of contact is unusual for miniaturized forms in which these bones typically exhibit extensive contact. On its posterior edge, the parietal presents a shallow nuchal fossa. Ventrally the parietal has an elongated decensus parietalis process that contacts the crista alaris of the prootic (Fig. 4C). The general shape of the main body of the parietal (i.e. excluding the postparietal process) can be described as a semicircle, given that both the anterior and the posterior margins are rounded. The anterolateral corner the parietal bears a small shelf that supports the posterolateral edge of the frontal in a hinge-like articulation along the mesokinetic axis. The postparietal process (ppp, Fig. 4A) originates laterally and diverges posteriorly. The distal portion of the postparietal process extends beyond the posterior margin of the parietal and contacts the squamosal posterolaterally and the base of the paroccipital process (pop, Fig. 4A,B) of the otooccipital.

The paired squamosal (sq, Fig. 4C) is a very reduced, bar-like, almost straight bone that is oriented at an angle of approximately 100° with relation to the longitudinal axis of the skull. This bone abuts the posterolateral surface of the postparietal process of the quadrate and is supported ventrally by the paroccipital process of the otooccipital and the quadrate.

The septomaxilla (smx, Figs 4B and 6) is a paired bone forming the floor of the air passage within the nasal cavity. The main body of this bone is shaped like a curved roofing tile with its concavity facing upwards. The septomaxilla contacts the maxillary lappet of the medial shelf anteriorly, the nasals dorsally and the vomer ventrally. In its medial portion, it bears a lateral process (smxlp, Fig. 6A,B) that extends to form a disk-like structure that faces forward. This process, combined with the vomer, forms the cupula Jacobsoni (cj, Fig. 6) and borders the nasal capsule (nc, Fig. 6) anteriorly. The septomaxilla reaches its highest point posterodorsally where a horn-like posterior process curves upwards.

The vomer (v, Figs 4B and 7A) is fused, although this fusion is incomplete at the anterior and posterior edges in some specimens. It contacts the maxillary lappet of the medial shelf anteriorly (mxl, Figs 4B and 7A), the septomaxillae dorsally and the palatine posteriorly. The premaxillary-vomer fenestra is absent and the premaxilla is excluded from the fenestra exochoanalis because the maxilla separates these bones. There is a small irregularly shaped notch anterior to the vomer which might be a remnant of this opening (Fig. 7A). In *Narudasia,* the vomer contacts the palatine via the two posterolateral processes of the vomer, which are reduced and oriented upwards, extending beyond the posterior margin of the bone itself to. This produces a more lateral contact of the vomer with the palatine; in other geckos, these posterolateral processes are wing-like projections that in some cases invade the choana, and the contact of palatine and vomer is more medial, closer to the intervomerine suture (Fig. 7B).

The palatine (pal, Figs 4A,B and 7A) is paired and of subequal width and length. It contacts the vomer anteriorly, the maxilla anterolaterally, the ectopterygoid laterally and the pterygoid posteriorly. It bears two anterior processes of approximately the same length – a medial vomerine process and a lateral maxillary process. The vomerime process contacts the posterolateral process of the vomer, and the lateral process contacts the medial shelf of the maxilla without overlapping it. The main body of the bone is roughly D-shaped, with a rounded medial edge and an almost straight lateral flange. At the base of the maxillary process is very tiny tubercle that contacts the ectopterygoid. The ventral surface of the palatine exhibits a shallow choanal canal. This bone curves downwards posteriorly, and at the posterior margin forms a transverse, mobile suture with the pterygoid with a looser contact medially than laterally. No observable pterygoid process was identified, so there is no tongue-in-groove articulation (Bell *et al.* 2003). Owing to the reduction of this contact between the palatine and the pterygoid, the skull is capable of a high degree of cranial kinesis (Versluys 1912; Frazzetta
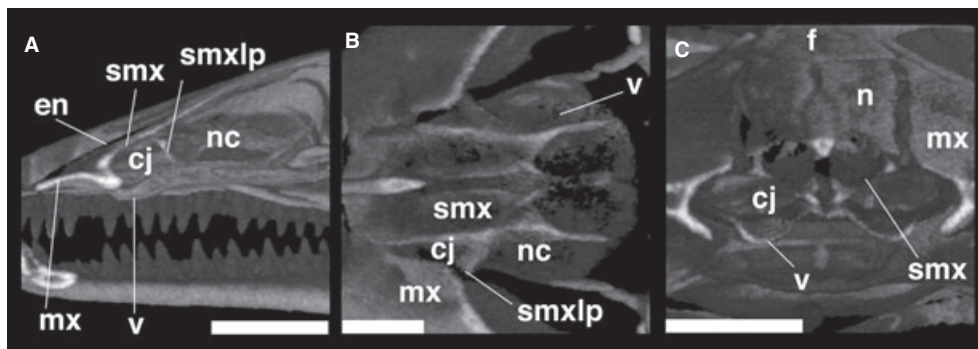

Fig. 6—Sagittal — **A**., horizontal — **B**. and coronal — **C**. Slices of *Narudasia festiva* (California Academy of Sciences 186278) snout showing septomaxilla. Abbreviations: cj, cupula jacobsoni; en, external nares; f, frontal; mx, maxilla; nc, nasal capsule; smx, septomaxilla, smxlp, lateral process of the septomaxilla; v, vomer. Scale bar equals 1 mm.
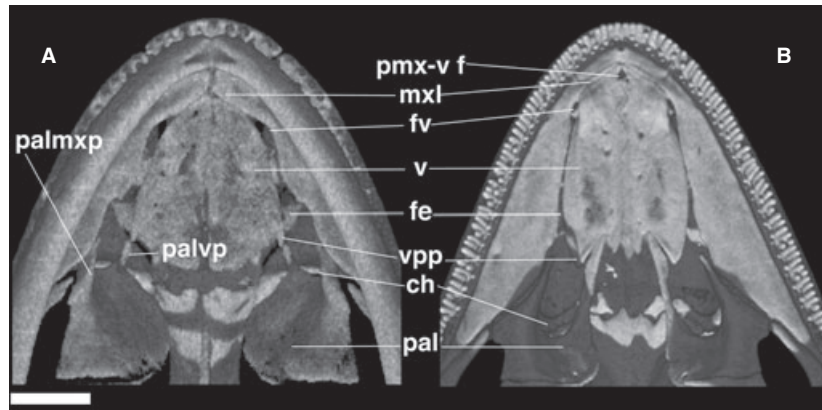
Fig. 7—Palatal view of the snout of — **A**. *Narudasia festiva* (California Academy of Sciences 186278) and — **B**. *Saltuarius cornutus* (Field Museum of Natural History 57503). Abbbreviations: ch, choana; fe, fenestra exochoanalis; fv, fenestra vomeronasalis; mxl maxillary lappet; pal, paltine; palmxp, maxillary process of palatine; palvp, vomerine process of palatine; pmx-v f, premaxillary-vomerine fenestra; vpp, posterolateral process of vomer. Scale bar equals 1 mm. *Saltuarius* palate not at the same scale.

1962; Rieppel 1984a). Anterolaterally, the palatine contacts the ectopterygoid, closing and forming the posterolateral margin of the suborbital fenestra. In the dorsal view, the posterior margin just reaches to the first third of the frontal, which gives the skull a very open appearance.

The pterygoid (pt, Fig. 4A,B) is a paired element with a Y-shape-like outline resulting from its bifurcated anterior margin and rounded indentation that defines the posterior margin of the suborbital fenestra. Anteriorly this bone has two processes, a longer and wider anteromedial process that contacts the palatines, forming a highly movable joint and a narrower and rod-like lateral process that is overlapped by the ectopterygoid. The articulation with the ectopterygoid is firm and excludes contact between the pterygoid and the maxilla or jugal. The medial margin of the pterygoid is sigmoidal and the lateral is concave. The fossa columella (fossa pterygoidei, Jollie 1960) is located approximately at half length of the bone and the epipterygoid inserts on it. The articulation of the pterygoid and epipterygoid in geckos is synovial, including a synovial cavity and surrounding fibrous capsule, as well as articular cartilage (Payne *et al.* 2011). Ventromedially to this articulation, the pterygoid participates in an additional synovial articulation with the basipterygoid; in geckos, the dorsal surface of the pterygoid is associated with the pterygoid meniscus which is abutted by the cartilaginous cap of the basypterygoid. These two cartilaginous processes lie within a cavity surrounded by a joint capsule composed of fibrous connective tissue (Payne *et al.* 2011). Posterolaterally, the pterygoid develops a syndesmosis with the medial surface of the quadrate (Payne *et al.* 2011); the posterior end of the pterygoid extends slightly beyond the articulation point. In the lateral view, the pterygoid is curved downwards behind the maxilla and it lacks the ventrolateral process.

The ectopterygoid (ect, Fig. 4A,C) is a paired, boomerang-shaped bone with both extremes tapering gradually to a point.

In the lateral view, its profile is wave-like because of the ventral pterygoid process and its slight posterior curve downwards. The ectopterygoid contacts the jugal laterally, and the pterygoid ventrolaterally via a small process, but without forming the dorsal process seen in other gekkotan species (Kluge 1962). Anteromedially, the ectopterygoid contacts the palatine, thus completing the suborbital fenestra. Thus, the suborbital fenestra is formed by the palatine anteromedially, the pterygoid posteriorly and the ectopterygoid laterally, the shape of this fenestra is oval and contrast with other species where it can be narrowed to a slit (Rieppel 1984a) or very large and D-shaped (Daza *et al.* 2008).

In *Narudasia*, there are 14 irregularly sized and shaped scleral ossicles, the ventral ones approximately twice as wide as the dorsal ones, arranged in an overlapping pattern, partially covering the eyeball. This number is typical for *Sphenodon* and many squamates (Gugg 1939; Romer 1956; Underwood 1970) and the most common count for both limbed geckos (Kluge 1967) and pygopodids (Underwood 1957), and has been interpreted as the ancestral state for gekkotans (Moffat 1973).

Splanchnocranium

The epipterygoid (ept, Fig. 4A,C,D) is a paired bar-like bone that is round in cross section and thickens slightly dorsally. It forms a synovial articulation with the pterygoid, inserting into the fossa columella and also articulating with the anterior surface of the crista alaris of the prootic; this articulation is a universal character among the Gekkonomorpha (Daza 2008) and has been reported as a synchondrosis in geckos, but the intimacy of this contact seems to be variable (see Payne *et al.* 2011 and references therein). The epipterygoid is oriented at a 75° angle with respect to the quadrate process of the pterygoid and nearly parallel to the quadrate.

The quadrate (q, Fig. 4) is a lightly built, streptostylic, shell-like bone that participates in the synovial craniomandibular articulation and that is connected to the braincase via a synchondrosis with the otooccipital (Payne *et al.* 2011). It also contacts the squamosal dorsally and the pterygoid ventromedially. The surface that forms the craniomadibular articulation is a smooth bicondylar surface capped with articular cartilage that bounds the synovial cavity dorsally. This part of the bone contacts the articular portion of the compound bone. The medial column is well developed and extends from the mandibular condyle to the cephalic condyle, which is positioned dorsomedially and forms a synchondrosis with the otooccipital (Payne *et al.* 2011). The quadrate has a large posterior concavity that accommodates the middle ear and provides surface for the attachment of the tympanic cartilage that supports the tympanic membrane (Hall 2005). The ossified dorsolateral surface has a deep square recess that is occupied by cartilage from which a styloid process extends ventrally. This may provide an additional support for the tympanic membrane and an indirect link between the stapes and the quadrate.

The stapes fits into the fenestra ovalis (fov, Figs 4C and 9D,F) with its oval footplate. Despite the small size of *Narudasia*, a stapedial foramen is present, as earlier noted by Bauer (1990a).

Neurocranium

The braincase is ossified into a single unit with discrete anterior orbitosphenoids. The rest of the braincase is the basicranium, which includes the parabasisphenoid (i.e. basisphenoid + parasphenoid), basioccipital, supraoccipital, prootic and otooccipital (i.e. opisthotic + exoccipital). These bones are completely fused and sutures are hard to distinguish or absent.

The ventral part of the braincase is formed by the parabasisphenoid and the basioccipital. The fusion between these two bones is complete and the sutures are absent or barely visible, which is an indication that the examined specimens are skeletally mature. Because of this fusion, we describe those portions assigned to each individual element based on descriptions where these bones have been disarticulated or have visible sutures (e.g. Oelrich 1956; Jollie 1960; Bever *et al.* 2005; Daza *et al.* 2008; Evans 2008). We describe the internal structures considering the braincase as a unit and using 3D digital endocasts as model (Bever *et al.* 2005; Olori 2010). The bones of the basal portion of the basicranium (parabasisphenoid and basioccipital) are more laminar than the remaining elements (prootic, otooccipital and supraoccipital), which are expanded to form the osseous labyrinth and the rest of the skeleton of the vestibular system.

The parabasisphenoid forms the anterior and ventral portion of the braincase. It contacts the pterygoid anterolaterally, prootic dorsally, and the basioccipital posteriorly. The parasphenoid portion bears the paired trabeculae (tbr, Fig. 8A), which are completely fused, forming a single anterior projection from which the cartilaginous cultriform projects anteriorly. The basipterygoid processes extends anterolaterally at a 45° angle with respect to the medial line. The basipterigoid is capped by pads of hyaline cartilage that are not significantly enlarged and that bound the medial side of the synovial cavity (Frazzetta 1962, Payne *et al.* 2011). A plate-like clinoid processes (clp, Fig. 8) that extends from the crista sellaris (crs, Fig. 8) of the parabasisphenoid overlays most of the basipterygoid process (except the articulation facets) and between these two structures is formed an enclosure
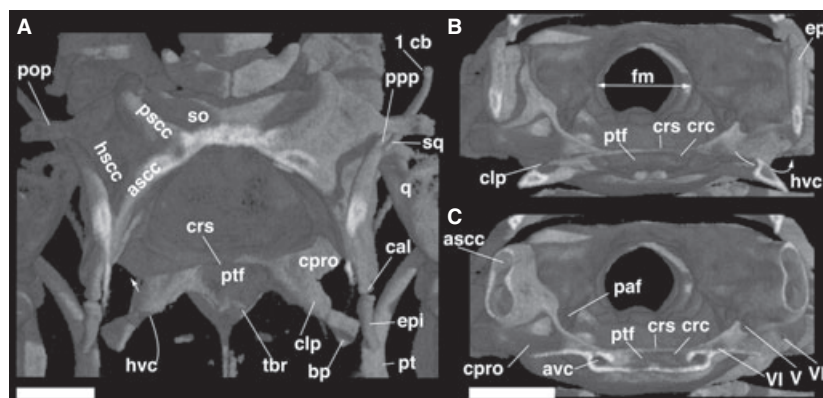

Fig. 8—Horizontal — **A**. and coronal — **B, C**. Slices of *Narudasia festiva* (California Academy of Sciences 186278), showing basicranial structures. Abbreviations: 1 cb, first ceratobranchial; V, incisura prootica for the course of the trigeminal nerve (cranial nerve V); VI, course for the abducens nerve (cranial nerve VI); ascc, anterior semicircular canal; avc, anterior opening of vidian canal; cal, crista alaris; clp, clinoid process; cpro, crista prootica; crs, crista sellaris; epi, epipterygoid; fm, foramen magnun; hvc, course for the lateral head vein; hscc, horizontal semicircular canal; pop, paroccipital process; ppp, postparietal process; pscc, posterior semicircular canal; pt, pterygoid; ptf, pituitary fossa; q, quadrate; sq, squamosal; tbr, trabeculae; q, quadrate; so, supraoccipital; sq, squamosal. Scale bar equals 1 mm.

for the course of lateral head vein (hvc, Fig. 8; Conrad and Norell 2007; Daza *et al.* 2008). A low, wide fossa for the pituitary gland (ptf, Fig. 8) lies behind the parasphenoid rostrum and is bordered by the crista sellaris posteriorly. Within this fossa are the paired carotid canals (crc, Fig. 8B,C) which are separated by a thin lamina from the wider anterior opening for the vidian canal (avc, Fig. 8C); these two canals are unusually close to each other when compared with other squamates, such as *Sphaeroactylus roosevelti* (Daza *et al.* 2008) and the gliptosaurine *Helodermoides tuberculatus* (Conrad and Norell 2008). A foramen for the abducens nerve (cranial nerve VI, Fig. 8C) is located at the base of the clinoid process, in a position between the anterior opening of the vidian canal and the incisura prootica. The posterior opening of the vidian canal or entocarotid fossa (pvc, Fig. 4B) appears as a ventrolaterally oriented pit that is positioned close to the base of the basipterygoid process. There is a fossa or sulcus that continues this opening and extends posterolaterally, forming the recesus vena jugularis (rvj, Fig. 9B), which is located ventral to the crista prootica.

The basioccipital contacts the parabasisphenoid anteriorly, the otooccipital laterally and the vertebral column (atlas) posteriorly. It forms the medial and ventral margin of the foramen magnun, and participates in the formation of the double occipital condyle, as in all gekkotans (Cope 1900; Gardiner

1982). As the basicranium is totally fused, it is unclear whether this bone participates in the formation of the occipital recess (ocr, Fig. 4B) or in the sphenoccipital tubercle.

The prootic forms the anterodorsal part of the basicranium, contacts the parabasisphenoid ventrally, the epipterygoid anteriorly, the parietal dorsally, the supraoccipital posterodorsally, and the otooccipital and stapes posteriorly. This bone is expanded mainly to accommodate the anterior and horizontal (lateral) semicircular canals and ampullae, and the anteriormost portion of the vestibule. The crista alaris (cal, Figs 4C and 9B) is well developed and is rounded directly upward, contacting the epipterygoid anteriorly and the parietal via thedecensus parietalis process (pdp, Figs 4C and 9B). Posterior to the crista alaris, the anterior semicircular canal (ascc, Fig. 9A) bulges and curves downward forming a loop and terminating in the anterior ampulla, which is twice the diameter of the anterior canal (aa, Fig. 9A). Contiguous with the anterior ampulla is the horizontal ampulla (ha, Fig. 9B) and horizontal semicircular canal (hscc, Fig. 9B) which extends posteriorly into the otooccipital. Lateroventral to this portion of the osseous labyrinth, the crista prootica is formed (cpro, Figs 4B, 8A and 9A,B), which in ventral view is triangular and well developed. The recessus vena jugularis (rvj, Fig. 9B) is ventral to the crista prootica and appears as an excavation posterior to the posterior opening of the vidian canal. The
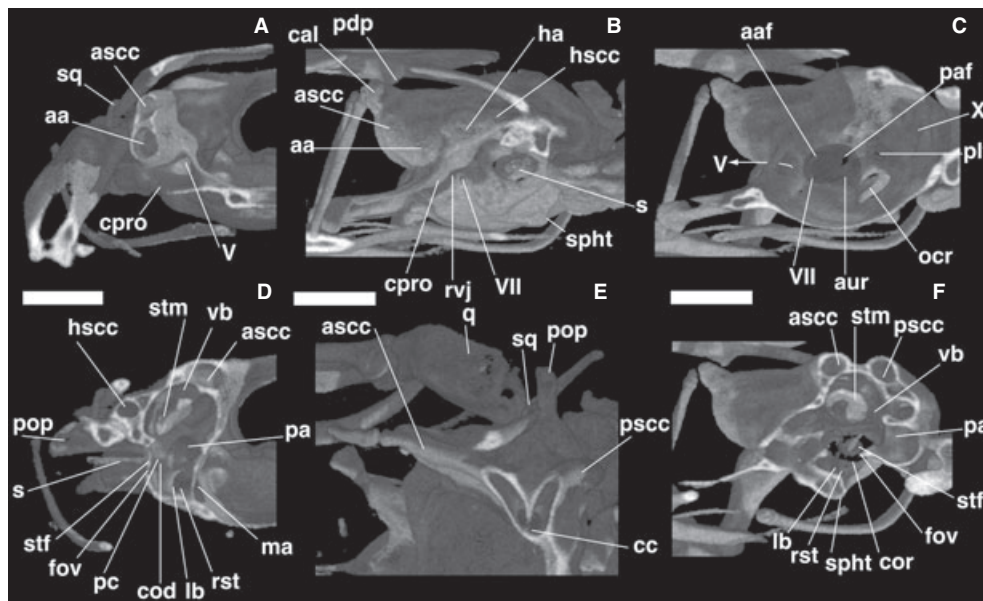

Fig. 9—*Narudasia festiva* (California Academy of Sciences 186278). — **A**. basicranium coronal cut of right side, — **B**., basicranium sagital cut showing the lateral left side, quadrate removed, — **C**. Basicranium sagittal cut showing the medial side right side. Abbreviations: V, incisura prootica for course of trigeminal nerve (cranial nerve V); VII, facial foramen; X, vagus foramen; aa, anterior ampulla; aaf, anterior acoustic foramen; ascc, anterior semicircular canal; aur, auditory recess; cal, crista alaris; cc, common crus; cod, cochlear duct; cor, cochlear recess; cpro, crista prootica; fov, fenestra ovalis, ha, horizontal ampulla; hscc, horizontal semicircular canal; lb, limbus, ma, medial aperture; ocr, occipital recess; pa, posterior ampulla; paf, posterior acoustic foramen; pc, perilymphatic cistern; pdp, decensus parietalis process; plf, perilymphatic foramen; pop, paroccipital process; pscc, posterior semicircular canal; q, quadrate; rst, recessus scala tympani; rvj, recesus vena jugularis; s, stapes; spht, sphenoccipital tubercle; sq, squamosal; stf, stapedial foramen; stm, statolithic mass; vb, vestibule. Scale bar equals 1 mm.

downward directed process that entirely encloses the incisura prootica or the path for the trigeminal nerve (cranial nerve V, Figs 8 and 9C) is visible in the medial wall of the braincase.

The facial foramen for the passage of cranial nerve VII pierces both the crista prootica and the lateral wall into the interior of the braincase (VII, Figs 8C and 9B,C) and is located in the inferior portion of a broad, deep auditory recess (aur, Fig. 9C) that accommodates the auditory ganglion. The septum intervestibulare is pierced by the anterior and posterior acoustic foramina (aaf, paf, Figs 8C and 9C; Conrad 2004). These foramina are unpaired and very wide, with the anterior one located dorsal to the facial foramen. The anterior acoustic foramen connects the auditory recess and the osseous labyrinth at the level of the anterior ampulla, transmitting vestibular branches of the vestibulocochlear nerve (VIII) to the semicircular canals (Bever *et al.* 2005). The posterior acoustic foramen connects with the auditory recess with the saccular portion of the vestibule.

The border between the prootic and the otooccipital is usually at the level of the fenestra ovalis (Kluge 1962; Daza *et al.* 2008), of which they form the anterior and posterior borders, respectively, although in *Narudasia,* the amount of participation of each bone in the margin of this fenestra is unclear. On the medial side, the separation of these two bones is probably located in the narrow area between the posterior edge of the acoustic recess and the perilymphatic foramen (plf, Fig. 9C).

The otooccipital forms the posterolateral part of the basicranium. It contacts the prootic and stapes anteriorly, the basioccipital ventrally, the supraoccipital dorsally and the quadrate and squamosal laterally. The paroccipital process (pop, Figs 4B and 9D,E) is long and strut-like, which is unusual for miniaturized forms, which typically have a stouter and less well-developed process. The anterior border of this process has a shallow depression, presumably to accommodate the quadrate and/or the adductor musculature. The paroccipital process extends horizontally and is connected to the epihyal via fibrous tissue. The ottooccipital and quadrate form a synchondroses (cartilaginous without a synovial cavity), the anterior surface of the paroccipital process contact the quadrate, a condition that has been described as suspension by 'paroccipital abutting' (Rieppel 1984a). Payne *et al.* (2011) did not find the quadrate–squamosal joint in five species representing four of the six families of fully limbed gekkotans (*Oedura lesueurii, Eublepharis macularius, Hemitheconyx caudicinctus, Tarentola annularis* and *Chondrodactylous bibronii*). We reviewed CT scan data for 23 gekkotans and found that the presence of this joint is variable (Table 1). In our sample, this articulation was absent in eight species. In some species (Table 1), a third element was present between the squamosal and the parietal, identified by Underwood (1957) as the supratemporal, this bone is not present in *Narudasia* (Fig. 9E).

The otooccipital portion of the braincase is broad and largely hollow, serving to accommodate the three osseous semicircular canals, the vestibule (vb, Fig. 9D) and the cochlear recess (cor, Fig. 9D). There is no clear division of these two

cavities in *Narudasia*, but based on endocast reconstructions and histological slices, the boundary between them is usually just below the level of the anterior and posterior ampullae, where a constriction is generally present (Wyeth 1924; Miller 1966; Olori 2010).

Details of the inner ear are not easily seen in our preparations, but the position of some of these parts can be determined based on the associated bony structures. The inner ear is divided into superior and inferior parts, termed the vestibule and cochlear recess, respectively (Hamilton 1960). The vestibule is the largest space of the inner ear and contains the sacculus and utriculus and is surrounded by the semicircular canals. It is bounded anteriorly by the anterior and horizontal ampullae in the prootic, and posteriorly by the posterior ampulla (pa, Fig. 9D,F). The vestibule contains a large statolithic mass (stm, Fig. 9D,F). As this calcareous condensation occupies most of the lumen of the sacculus, it is possible to infer the position and shape of this membranous structure (Baird 1960; Olori 2010). In *Narudasia*, it resembles a biconcave disk. Medial to the sacculus is a large space that is occupied by the utriculus (Shute and Bellairs 1953). The spaces occupied by the sacculus and the utriculus are comparable in size in *Narudasia*. From the sacculus the endolymphatic duct arises, passing through the endolymphatic foramen in the supraoccipital (Oelrich 1956; Kluge 1967; Baird 1970) and expand into the endolympatic sacs, which are extracranial structures that lie along the surface of the cervical musculature (Wiedersheim 1875; Kluge 1967; Bauer 1989). The opening for the endolymphatic duct in *Narudasia* is located between the parietal and the supraoccipital as has been reported for other geckos (Häupl 1980). Both the sacculus and the utriculus are connected by a short sacculo-utricular duct (Hamilton 1960, 1964). The cochlear duct is a diverticulum of the sacculus that is contained in the cochlear recess (cor, Fig. 9D,F). The saccule and the cochlear duct are connected via a narrow constriction or sacculo-cochlear duct (Wyeth 1924; Olori 2010). The cochlear recess is located at the level of the fenestra ovalis and the stapes, (fov, stf, Figs 4C and 9D). In addition to the cochlear duct, the cochlear recess contains two perilymph-filled regions, the scala vestibuli and scala tympani, which are connected through a perilymphatic duct that curves around the anterior margin of the cochlear duct (Hamilton 1960, 1964; Freeman 1990). The space immediately medial to the footplate of the stapes and the fenestra ovalis (stf, fov, Fig. 9D) is occupied by the perilymphatic cistern (pc, Fig. 9D), which has an anteriorly directed extension or scala vestibule.

In the CT scan, a faintly outlined structure in the vicinity of the medial wall of the cochlear duct corresponds to a poorly ossified limbus (lb, Fig. 9D,F). The limbus may be divided in two parts, the neural limbus (which houses the cochlear nerve) and the abnerual limbus cartilage (Ganeshina and Vorobyev 2009); compared with other lizards, gekkotans have a very distinct limbus, which develops an extensive hook-shaped lip, this defines an inverted U-shaped

Table 1 Presence of quadrate–squamosal joint and supratemporal bone in 32 species of gekkotans. See Materials and Methods for collection acronyms

	Family	Species	Quadrate–squamosal joint	Supratemporal
Pygopodoidea	*Insertae sedis*	*Gobekko cretacicus* (ZPAL MgR-II⁄4)	?	Y?
	Carphodactylidae	*Nephrurus asper* (California Academy of Sciences (CAS) 74733)	Y	N
		Saltuarius cornutus (Field Museum of Natural History (FMNH) 57503)	Y	N
	Diplodactylidae	*Eurydactylodes vieillardi* (CAS 231986)	N	N
		Rhacodactylus auriculatus (CAS 205486)	Y	N
		Strophurus ciliaris (FMNH 215488)	N	N
	Pygopodidae	*Aprasia repens* (CAS 104382)	-	N
		Delma borea (USNM 128679)	N	N
		*Lialis burtonis (*FMNH 166958)	N	N
Gekkonoidea	Eublepharidae	*Aeluroscalabotes felinus* (FMNH 146141)	N	Y
		Coleonyx variegatus (YPM 14383)	N	N
		Eublepharis macularius (CM 67524)	N	Y
	Sphaerodactylidae	*Aristelliger georgeensis* (CAS 176485)	Y	N
		Gonatodes albogularis (FMNH 55929)	Y	N
		Pristurus carteri (CAS 225349)	Y	N
		Teratoscincus przewalskii (CAS 171013)	N	N
	Gekkonidae	*Afroedura karroica* (CAS 198274)	Y	N
		Agamura persica (CAS 140562)	Y	N
		Cryptactites peringueyi (CAS 186375)	Y	Y
		Cyrtodactylus ayeyarwadyensis (CAS 221985)	Y	N
		Gekko gecko (AMNH R-140787)	Y	N
		Goggia lineata (CAS 193627)	Y	N
		Hemidactylus frenatus (CAS 215743)	Y	N
		Lygodactylus capensis (CAS 167621)	-	N
		Narudasia festiva (CAS 186278)	Y	N
		Pachydactylus bicolor (CAS 223912)	Y	N
		Phelsuma lineata (Museum of Comparative Zoology 11691)	N	N
		Ptenopus carpi (CAS 214548)	Y	N
		Rhoptropus afer (CAS 193865)	Y	N
		Tropiocolotes helenae (CAS 120795)	N	Y
		Uroplatus fimbriatus (CAS-SU 13469)	Y	N
	Phyllodactylidae	*Gymnodactylus geckoides* (CAS 49397)	N	N

structure that encloses an ample cochlear sulcus and serves as the attachment for the tectorial membrane (de Burlet 1934; Shute and Bellairs 1953; Underwood 1957; Ganeshina and Vorobyev 2009). The neural limbus has a gap, termed the limbic hiatus (Hamilton 1960), which serves as a frame for the basilar membrane; this could be corroborated in sagittal and coronal sections of the CT scan. In gekkotans, the abneural limbus cartilage is partially replaced by a noncartilaginous contractile segment (Ganeshina and Vorobyev 2003, 2009).

Medial to the basilar membrane is the perilymphatic foramen, leading into perilymphatic sac, which is housed in the recessus scala tympani (rst, Fig. 9D,F), which in lizards is represented by the occipital recess (ocr, Figs 4B and 9D; Oelrich 1956; Rieppel 1985). This recess has one connection with the brain cavity into a submeningeal space through the medial aperture (ma, Fig. 9D; a.k.a. cochlear aqueduct) and one external connection towards the pharyngeotympanic cavity by means of the fenestra rotunda (=apertura lateralis recessus scalae tympani).

Mandible

The mandible is composed of five discrete elements, the dentary, coronoid, splenial, surangular and a compound bone (Fig. 10). The last of these elements is often interpreted as a fusion of the angular, prearticular and articular.

The dentary has 25–27 tooth loci. This bone is elongated and tubular, containing the closed Meckelian canal (mk, Fig. 11). It articulates extensively with its fellow in the ventral midline to form a mostly horizontal mandibular symphysis (sy, Fig. 4B). Posteriorly, this bone contacts all the postdentary bones at some point, including the compound bone. In the labial view, there are three processes: a posterodorsal coronoid process (cop, Fig. 10A) and a subcoronoid process (scop, Fig. 10A) of the same length, and the longer angular process, which extends beyond the coronoid eminence (ap, Figs 10C and 11). The labial surface of the dentary is pierced by 2–4 mental foramina (mf, Fig. 10A).

The splenial contacts the dentary, coronoid and the compound bone (spl, Fig. 10A). Its anterior margin is widened,
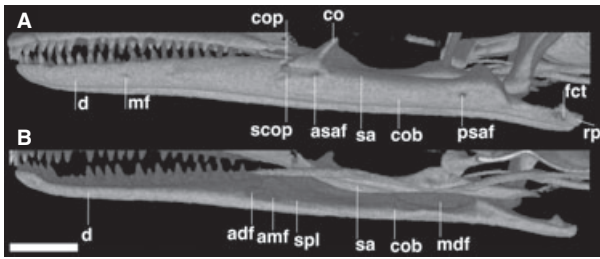
Fig. 10—*Narudasia festiva* jaw (California Academy of Sciences 186278) in — **A**. labial and — **B**. lingual views. Abbreviations: adf, anterior inferior dental foramen; amf, anterior mylohyoid foramen; ap, angular process; asaf, anterior surangular foramen co, coronoid; cob, compound bone; cop, posterodorsal coronoid process; d, dentary; fct, foramen for the chorda tympani; mdf, mandibular fossa; mf, mental foramina; psaf, posterior surangular foramen; rp, retroarticular process; sa, surangular; scop, subcoronoid process; spl, splenial. Scale bar equals 1 mm.
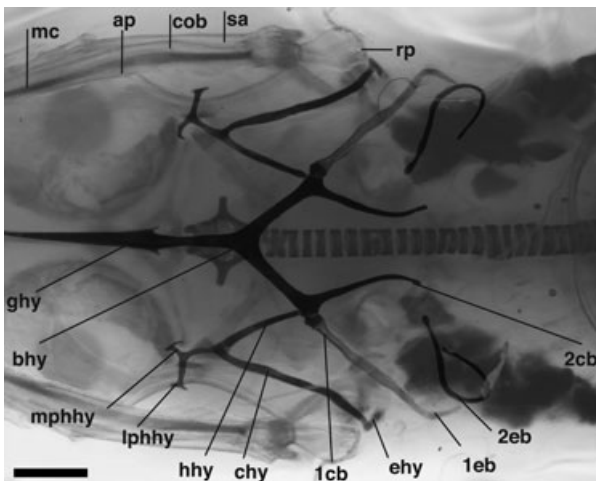

Fig. 11—*Narudasia festiva* (California Academy of Sciences 186290) showing the complete hyoid apparatus. Abbreviations: 1 cb, first ceratobranchial; 1 eb, first epibranchial; 2 cb, second; ap, angular process; bhy, basihyal; chy, ceratohyal; cob, compound bone; ehy, epihyal; ghy, glossohyal; hhy, hipohyal; lphy, lateral projection of hipohyal; mc, Meckel cartilage; mphy, medial projection of hipohyal; rp, retroarticular process; sa, surangular. Scale bar equals 1 mm.

whereas the posterior portion tapers, forming a long suture with the dentary. It forms the anteromedial wall of the Meckelian canal. The splenial is pierced by two discrete oval foramina, the anterior inferior dental foramen and the anterior mylohyoid foramen (adf, amf, Fig. 10B), the former being twice the diameter of the latter.

The coronoid is a triangular-shaped bone that clasps the dentary anteriorly and contacts the surangular and the compound bone posteriorly (co, Figs 4C and 10A). Its anterolingual process is flat and directed towards the anterior inferior dental foramen. The dorsal coronoid process is rather high

and pointed, extending above the contour of the jaw (Fig. 10A). Its posterior shelf is very narrow and has almost no overlap with the surangular.

The surangular remains as a discrete element and firmly overlies the compound bone ventrally. The dentary processes inserts into the Meckelian canal, and together with the compound element, constitutes the main brace for the dentary. The coronoid and the compound bone continue the Meckelian canal posteriorly to the mandibular fossa (mdf, Fig. 10B). The anterior surangular foramen is very conspicuous and lies between the coronoid and the surangular (asaf, Fig. 10A). The posterior surangular foramen (psaf, Fig. 10A) pierces this bone in the basal portion of the cranio-mandibular articulation. The contact of the surangular is almost at the same antero-posterior level as coronoid-dentary suture.

The compund bone forms, together with the surangular, the mandibular fossa. The mandibular fossa opens labially through the posterior surangular foramen. The articular portion is very wide and flat. Posteriorly, a wide spoon-shaped retroarticular process (rp, Figs 4B,C, 10A and 11) is developed. This process is narrow at the base and is oriented mostly posteriorly and pierced by the foramen for the chorda tympani (fct, Fig. 10B).

Hyoid apparatus

In the cleared-and-stained the preparations, the elements of the hyoid skeleton were stained predominantly by the alcian blue with a mixture of alizarin red. Parts of the hyoid were also revealed by the two types of X-ray preparations, indicating that these elements are partly ossified, although they do not ossify completely, even in adult *Narudasia* (Bauer 1990a).

Narudasia has all the typical elements of the lizard hyoid apparatus (Noble 1921; Oelrich 1956; Stephenson and Stephenson 1956; Jollie 1960; Kluge 1962; Bauer 1990b). The glossohyal (ghy, Figs 4B and 10, a.k.a. lingual process) resembles a Roman dagger. The glossohyal runs ventral and almost parallel to the cultriform process. The basihyal (bhy, Figs 4B and 11) is bifurcated posteriorly, and three elements arise from each one of its posterior ends: the anterior hipohyal (hhy, Figs 4B and 10D), posterolaterally the robust first ceratobranchial (1cb, Figs 4B and 10D), and a posteromedially the second ceratobranchial (2cb, Figs 4B and 11). The anterior end of the hypohyal (a.k.a. hyoid cornu) has medial and lateral projections (mphy and lphhy, Fig. 11) which, together with the last segment of the hypohyal, create a Y-shaped structure that resembles a serif typeface. From the base of this Y-shaped structure, the ceratohyal (chy, Fig. 11) arises and articulates with the cartilaginous epihyal (ehy, Fig. 11); the epihyal develops a connection with the basicranium at the paroccipital process. The most robust and cylindrical portion of the hyoid apparatus is the first ceratobranchial (1cb, Fig. 11), which is the only element that shows complete ossification. This element articulates with the first epibranchial (1eb, Fig. 11). The first epibranchial curves upwards

passing the posterior part of the basicranium and is positioned behind the quadrate. The second ceratobranchial (2cb Fig. 11) is well developed, and most of the structure is oriented medially but at the distal end it is curved towards the independent second epibranchial (2eb Fig. 11).

Postcranium

The postcranium (Fig. 12) of *Narudasia festiva* constitutes approximately 85% of the entire body length, with subequal body and the tail sections. The vertebral column is composed of 25 presacral, two sacral and about 19–22 caudal vertebrae. Centrum morphology is amphicoelous and an intercentrum is firmly attached intervertebrally but not fused to any of the vertebrae. The presacral region comprises eight cervicals, 15 thoracics and two lumbars. In the cervical region, the atlas, axis and the third cervical are ribless, and the remaining five cervicals bear ribs that increase in length gradually. The atlas is characterized by unfused neural arches. The atlas has two short, rounded posterior projections that do not overlie the axis. The 4th cervical has short ribs that are bifurcated distally, but only weakly expanded. The ribs of the 5th–8th cervicals approach the suprascapular element of the pectoral girdle. The 8th cervical rib is well separated from the sternum. The sternal ribs (stnr, Fig. 13) of the first three thoracic vertebrae are attached to the sternum directly (Fig. 13). The 4th thoracic rib is attached via the xiphisternum (xy, Fig. 13). The remaining thoracic vertebrae articulate with long ribs that are associated with very small postxiphisternal inscriptional ribs that gradually reduce in size posteriorly. The longest ribs are present on the 8th and 9th thoracic vertebra; more posteriorly the ribs decrease in size gradually and become arched anteriorly. The two lumbar vertebrae are similar to the posterior thoracic vertebrae but more expanded than the anterior thoracic vertebrae. The anterior sacral vertebra has very long transverse processes with expanded articular facets for the
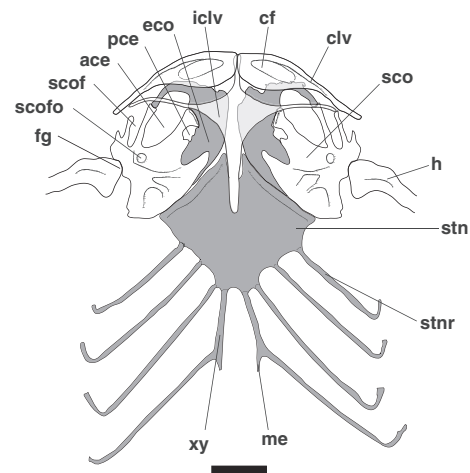
Fig. 13—Pectoral girdle of *Narudasia festiva* (California Academy of Sciences 186290). Abbreviations: ace, anterior coracoid emargination; cf, clavicular fenestra; clv, clavicle; eco, epicoracoid; fg, fossa glenoidea; h, humerus; iclv, interclavicle; me, mesosternal extension; pce, posterior coracoid emargination; sco, scapulocoracoid; scof, scapulocoracoid fenestra; scofo, scapulocoracoid foramen; stn, sternum; stnr, sternal rib; xy, xiphisternum. Scale bar equals 1 mm.

pelvic girdle (ilium) and posteriorly it is partially fused to the anterior part of the bifurcated transverse processes of the second sacral. The transverse process of the second sacral exhibits a foramen before to the bifurcation point. The precise total number of caudals could not be determined because none of the specimens examined osteologically had a complete tail, but a rough estimation is 19–22. The first five caudal vertebrae are short and square, lack autotomy planes, and have long transverse processes that decrease in size gradually distally. The last transverse process is curved posteriorly. The pygal series (those with no hemal arches, sensu Russell 1967; not caudals free of fracture planes, sensu Holder 1960) is
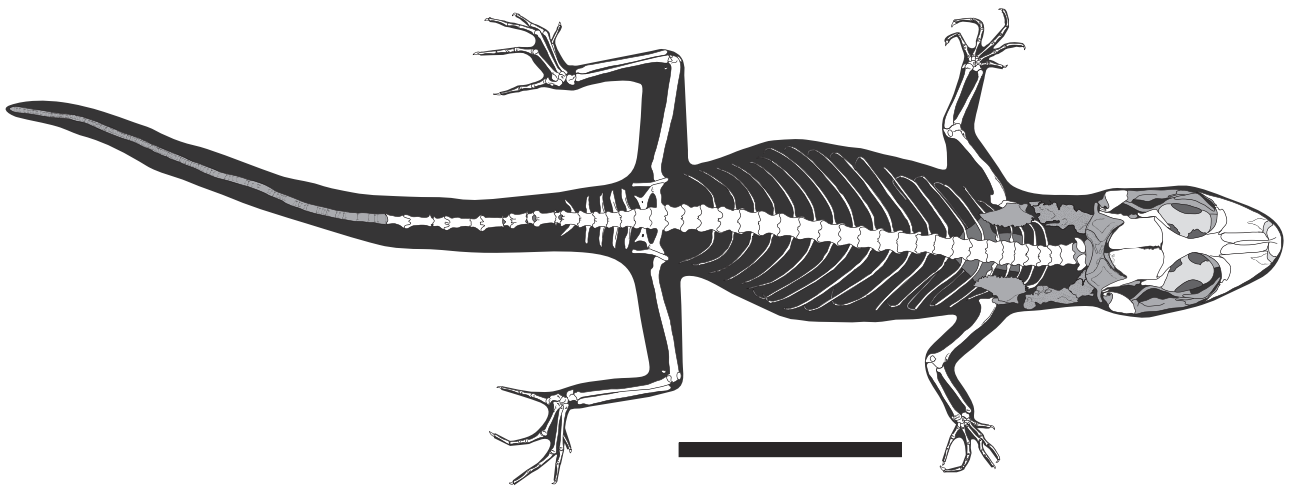
Fig. 12—Complete skeleton of *Narudasia festiva* (California Academy of Sciences 186290). Scale bar equals 10 mm.

formed only by the three-first caudals. The 6th caudal vertebra is the first with an autotomy plane. The autotomy septum lies immediately distal to the transverse process, in a more anterior position than in other gekkonids, such as *Christinus marmoratus* (Kuhn *et al.* 2008). Caudal autotomy occurs most commonly in the 6th vertebra, although some specimens had autotomized in the 10th, 11th (Fig. 12), 14th, or even the 22nd vertebra. Beyond the 6th vertebra, the caudal vertebrae elongate gradually and some are three times as long as those at the base of the tail. Distal caudal vertebrae are more cylindrical in overall shape and have reduced transverse processes, with greatly expanded and laterally flared postzygapophysis.

The pectoral girdle is composed of paired suprascapulae, scapulocoracoids, epicoracoids, and clavicles, and the unpaired interclavicle and sternum (Fig. 13). The suprascapulae, epicoracoids and sternum were stained by both alcian blue and alizarin red, indicating partial ossification. The suprascapula is greatly expanded with an irregular edge (Fig. 12). The scapular portion of the scapulocoracoid (sco, Fig. 12) is short and stout (length less than three times its distal width). The scapulocoracoid fenestra (scof, Fig. 13) is present and emarginated anteriorly. Anterior and posterior coracoid emarginations (ace and pce, Fig. 13) are present, but the posterior is less well developed. The clavicles (clv, Fig. 13) are greatly expanded medially and horizontally oriented with well-defined clavicular fenestra (cf, Fig. 13). The clavicles articulate in the midline and contact the interclavicles dorsally. The interclavicle (iclv) is cruciform and has very elongate lateral arms that are in contact with the clavicles. The interclavicle inserts up to half the total sternum length, a greater intrusion into this element than reported by Kluge and Nussbaum (1995). The sternum (stn, Fig. 13) is shield-like and has an unbranched xiphisternum with a mesosternal extension (me, Fig. 13).
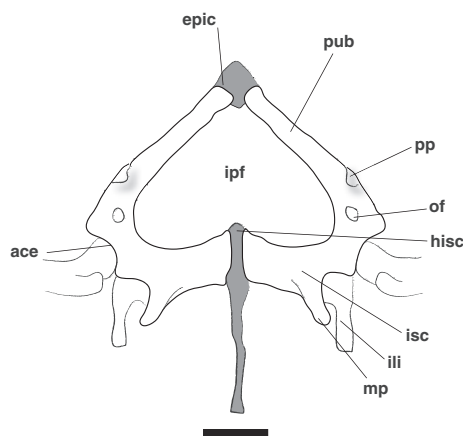

Fig. 14—Pelvic girdle of *Narudasia festiva* (California Academy of Sciences 186290). Abbreviations: ace, acetabulum; epic, epipubic cartilage; hisc, hipoischum; ili, ilium; ipf, schiopubic fenestra; isc, ischium; mp, metischial processes; of, obturator foramen; pp, pectineal process; pub, pubis. Scale bar equals 1 mm.

The pelvic girdle is formed by the fusion of the ilium, ischium and pubis (Fig. 14). The ilium is rod-like and firmly contacts the transverse process of the first sacral vertebra (Fig. 12). The pubis and the ischium form a spade-shaped ischiopubic fenestra (ipf, Fig. 14), different from the inverted heart shape as in the diplodactylid gecko *Bavayia sauvagii* (Bauer 1990b). This shape is determined mostly by the symphyseal portion of the pubis (pub, Fig. 14), which is long and strut-like, whereas the tubercular portion is very short. The pubis does not form a symphysis with its fellow, but rather contacts an enlarged and wedge-shaped epipubic cartilage (epic, Fig. 14) anteriorly. The pubis has a domed pectineal process and is pierced by the obturator foramen (of, Fig. 14). The ischium is twice the width of the pubis and has two finger-like metischial processes (mp, Fig. 14) that are directed posterolaterally and widely separated from each other. Like the pubis, the ischia are separated in the midline, in this instance by an elongated cartilaginous hypoischium (hisc, Fig. 14), which extends from the posterior border of the ischiopubic fenestra to the anterior edge of the cloaca.

The limbs are long and slender and all of the elements of the typical gecko appendicular skeleton (Fig. 12; Russell 1972; Russell and Bauer 2008) are present. The forelimb is 70% the length of the hindlimb. The percentage of each forelimb subdivision in the specimen illustrated is: stylopodium (humerus) 40.1%, zeugopodium (radius, ulna) 28.6%, and autopodium (carpus, metacarpal and digit III) 31.3%. For the hindlimb, these values are as follows: stylopodium (femur) 37.2%, zeugopodium (tibia, fibula) 29.5% and autopodium (tarsus, metatarsal and digit III) 33.3%.

The humerus is long and slightly bowed, its preaxial tuberosity is squarish in profile and its deltopectoral crest is continuous with the bone surface. The ectepicondyle is laminar and has a noticeable ectepicondilar foramen. The medial surface of entepicondyle is smooth, and the fossa formed behind the capitulum and the trochlea is deep. There are no sesamoids between the humerus and the radius or the ulna, but the ulnar patella is well developed and located dorsally to the humerus. The ulna articulates distally with the pisiform, the ulnare and the radiale and the radius contacts the radiale posteriorly. The carpus exhibits a typical rosette arrangement with a centrale at its core, surrounded by the ulnare, radiale and distal carpals 1–5. The radiale is bulkier than the ulnare and is in contact with the ulna, ulnare, centrale, distal carpal 1 and metacarpal 1. Metacarpal 1 is the shortest; metacarpals 2–5 are subequal to the penultimate phalanges. The phalangeal formula of the manus is 2-3-4-5-3.

The femur is straight and its head is perpendicular to the acetabulum so the zeugopodium is oriented mostly horizontally with only a minor downward inclination. The internal trochanter is strongly developed and the distal condyles are confluent with a deep intercondylar fossa. There are four sesamoids in the knee joint area: (1) the tibial patella, which is mostly dorsal to the femur, (2) the ventral pre-axial tibiofemoral lunula between the femur and the tibia, (3) one

between the femur and the fibula and ventral to the proximal fibular epiphysis and (4) one behind the knee and corresponding to the post-axial ligament. An additional sesamoid, the fabella, is embedded in tendon of the flexor gastrocnemius femoralis superficialis muscle (Jerez *et al.* 2010). The tarsus comprises two bones, the fused astragalus and calcaneum in contact with the tibia and fibula and a smaller, laterally located cuboid. The cuboid articulates with the astragalo-calcaneum and the metatarsals. Metatarsal 5 is the smallest and is slightly hooked, producing a fifth pedal digit that is opposable to the metatarsals 1–4, which are almost parallel. In increasing order, the relative length of the metatarsals is 5-4-1-2-3. The pedal phalangeal formula is 2-3-4-5-4.

Discussion

Narudasia has been allied by previous workers to the gekkonids *Stenodactylus*, *Tropiocolotes*, *Calodactylodes*, and *Rhoptropus*, to the phyllodactylid *Homonota*, and to the sphaerodactylid *Quedenfeldtia* (see Introduction; Parker (1936) suggested affinities to *Gymnodactylus* as well, but his concept of this genus would have included geckos currently placed in at least six genera in the families Gekkonidae and Phyllodactylidae), but in most cases, such interpretations have been based on overall appearance rather than any explicit morphological similarities.

Despite previously proposed similarities to genera now grouped in other gekkotan families, molecular phylogenetics strongly supports the inclusion of *Narudasia* within the Gekkonidae *sensu stricto* (Feng *et al.* 2007; Gamble *et al.* 2008a,b). Unfortunately, to date no unambiguous morphological synapomorphies of the Gekkonidae, Sphaerodactylidae, or Phyllodactylidae have been identified and, as these three families together form a natural group within Gekkota; any similarities between *Narudasia* and some subset of other genera within this clade might only reflect symplesiomorphies.

Although relationships within the Gekkonidae remain incompletely resolved, there is support for a broad Afro-Malagasy clade, including virtually all southern African gecko genera as well as most of those occurring on Madagascar and other Indian Ocean islands (Gamble *et al.* 2011; Bauer A.M., unpublished data). Both *Ptenopus*, another southern African endemic gekkonid, and *Narudasia* are relatively basal, long-branched representatives of this clade, whereas *Rhoptropus* is nested deep within it in a broader group including *Pachydactylus* and its satellite genera (Bauer and Lamb 2005). Of those genera previously linked to it, *Narudasia* shares the greatest number of cranial osteological similarities with *Rhoptropus* (Fig. 15A,B), including the presence of a small depression in the postnarial area (mxd, Fig. 15C,D). However, these two taxa differ in the length of the ascending nasal process of the premaxilla and nasal bones (asnp and n, Fig. 15A); the latter are about 70% the length of the frontal bone in *Narudasia*. Further, *Narudasia* lacks the hyperphalangy of digit I that characterizes *Rhoptropus* and its close relatives. Haacke (1976)
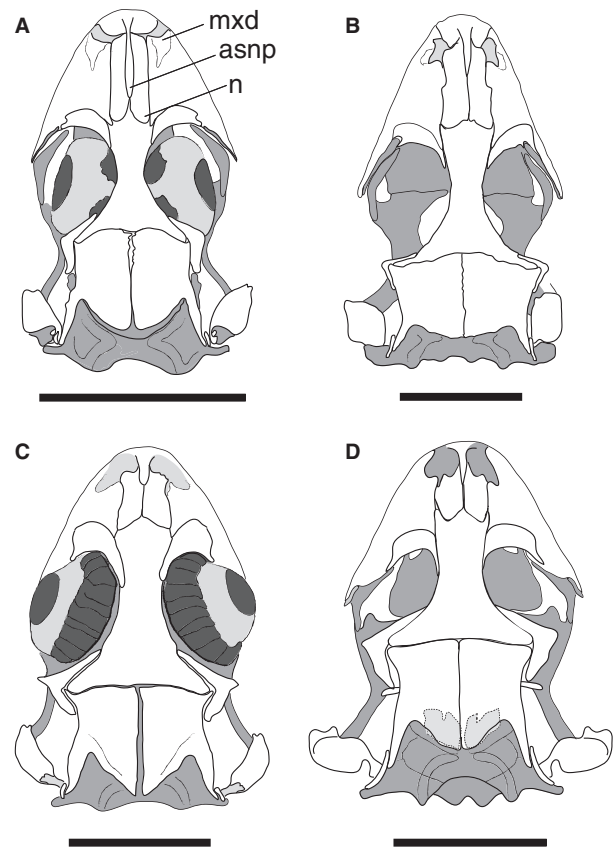

Fig. 15—Dorsal view of skulls of — **A**. *Narudasia festiva* (California Academy of Sciences (CAS) 186290), — **B**. *Rhoptropus afer* (BMNH 1937.12.3.60), — **C**. *Stenodactylus sthenodactylus* (CAS 132688) and — **D**. *Homonota fasciata* (FML 01495), (C). Abbreviations: asnp, ascending nasal process; mxd, anterodorsal depresion of maxilla; n, nasal. Scale bar equals 5 mm. [Corrections added after online publication (July 20, 2011): Fig 15 replaced with new figure.]

reported that the manual phalangeal formula of *Narudasia* was 2 : 3 : 4 : 5 : 4, thus representing a case of hyperphalangy of digit V. This condition has not subsequently been confirmed (e.g. Bauer 1990a; Russell and Bauer 2002, 2008), and all specimens examined as part of this study retain the primitive phalangeal formulae for both the manus and pes (2 : 3 : 4 : 5 : 3 and 2 : 3 : 4 : 5 : 4, respectively). On this basis, it seems unlikely that *Narudasia* shares immediate ancestry with *Pachydactylus* and *Rhoptropus* as these two genera present manual and pedal phalangeal formulas of 3 : 3 : 4 : 5 : 3 and 3 : 3 : 4 : 5 : 4, respectively.

An alternative explanation for similarities between *Narudasia* and apparently unrelated gekkotans is miniaturization, which may result in convergent characters that obscure phylogenetic relationships. Miniaturization has occurred in several lineages across the Squamata, including the Gekkota, which includes the smallest amniote (Hedges and Thomas 2001). The very small size of *Narudasia* qualifies it as a miniaturized lineage and, as such, constraints on skeletal morphology,

particularly that of the skull, might be expected to result in its convergence or parallelism with other miniaturized taxa. Indeed, of those genera associated with *Narudasia* in the past, *Calodactylodes*, *Rhoptropus* and *Stenodactylus* are the only groups not generally regarded as miniaturized lineages. Daza (2008) reviewed the distribution of 17 cranial characters that have previously been associated with miniaturization and these have here been evaluated for *Narudasia*.

Narudasia, *Tropiocolotes*, *Homonota* and the sphaerodactyl geckos have the general characters associated with miniaturization seen in other squamate groups, such as a large neurocranium relative to the dermatocranium (Rieppel 1984b, 1996) and a bulging occipital condyle (Daza *et al.* 2008). However, many other features typical of at least some miniaturized forms are not found in *Narudasia*; for example, one common consequence of a large basicranium is the closure of the postemporal fossae (formed by the postparietal process of the parietal, the squamosal and the braincase Rieppel 1984b); however, this does not occur in *Narudasia* or *Tropiocolotes*, where these fossae remain open.

The basipterygoid and paroccipital processes are stout in miniaturized sphaerodactyls and *Tropiocolotes*, but in *Narudasia*, these two processes are slender and elongated. The paroccipital process has multiple functions in the skull: it has an important role in the support of the quadrate dorsally in many lizards (Rieppel 1984a; Estes *et al.* 1988), may be connected with the stapedial apparatus by a ligament (McDowell 1967) and can also serve as a surface for the insertion of the neck muscles the *m. obliquus capitis*, *m. longissimus cervicis* and *m. episternocleidomastoideus* (Oelrich 1956; Al Hassawi 2007).

The arrangement of the dermatocranial bones of the muzzle unit in *Narudasia* differs from that found in miniaturized sphaerodatyls, most pygopodids (Kluge 1976; Rieppel 1984a; Daza *et al.* 2008), and *Homonota*. In these taxa, the snout is short; for this reason, the frontoparietal suture is located at the midpoint along the total length of the skull. *Narudasia*, *Tropiocolotes* and *Quedenfeldtia* muzzle: parietal unit ratio of approximately 2 : 1, as is typical of larger gekkotans (Daza *et al.* 2008, 2009). However, in contrast to larger forms, the muzzle bones of *Narudasia* exhibit a high degree of overlap. The shape of the dorsal process of the maxilla also differs between *Narudasia* and the sphaerodactyls; in *Narudasia*, the posterior edge of the dorsal process is more concave and overlaps extensively the prefrontal like in all other gekkotans used as comparison, except sphaerodactyls, which have a more rectangular process, leaving exposed an anterior portion of the prefrontal.

Tropiocolotes and *Homonota* share with *Narudasia* an occipital recess that is totally visible in ventral view (i.e. not hidden by the spheno-occipital tubercle), and *Quedenfeldtia* and *Homonota* share with *Narudasia* a broadening of the retroarticular process. However, these other genera differ from *Narudasia* in having an obtuse dorsal process of the maxilla that does not separate the frontal and prefrontal anteriorly, a bony contact of the parietal and the supraoccipital, and

ventral contact of the crista alaris and the epipterygoid; Additionally, *Quedenfeldtia* and *Homonota* exhibit some sculputuring of the dermal bones, a trait not seen in *Narudasia*. The frontal bone is also less stout in *Narudasia* than in *Stenodactylus* (Fig. 15C) and *Homonota* (Fig. 15D). Further, these two genera, as well as *Ptenopus*, differ from *Narudasia* in having vaulted snouts, a W-shaped nasofrontal suture, the frontal bone with dagger-shaped anterolateral processes, a transverse frontoparietal suture, and surangular-dentary contact posterior to coronoid-dentary suture.

In *Narudasia*, the frontal bone has smaller crista cranii anterior processes which are positioned closer to each other than in *Sphaerodactylus roosevelti*. The parietals also differ in shape, being more rectangular in *Sphaerodactylus* and semicircular in *Narudasia*. The latter also has a longer postparietal process.

The quadrate foramen in *Narudasia* is located in a medial position, while in *S. roosevelti*, this foramen is just dorsal to the mandibular condyles. Similar variation has been is seen among the different sphaerodactyl genera (Daza *et al.* 2008).

The mandible of *Narudasia* has a larger compound bone, and coronoid, than in sphaerodactyls. In the former, the coronoid is high, triangular and somewhat pointed. A similar coronoid is present in *Homonota*, but in *Tropiocolotes* and sphaerodactyls, this bone is very low and does not extend too much from the jaw outline. The external mandibular fenestra is rounded and much smaller in *Narudasia*. It is also located further posteriorly than in *Sphaerodactylus*.

The palate of *Narudasia* is also very distinct from other miniaturized geckos, such as the spaherodactyls (Daza *et al.* 2008); for instance, in *Narudasia*, the premaxilla does not contact the vomer, and the maxilla does not exhibit the extensive ventral overlap of the premaxilla that is widespread across gekkotans. Instead there is extensive medial contact of the maxillary lappets of the maxilla, a character that has been considered as derived for gekkotans (Rieppel 1984a; Kluge 1995; Kluge and Nussbaum 1995) and has been recorded in *Rhoptropus afer*, *Ptenopus carpi*, and *Pristurus carteri* (Häupl 1980; Kluge 1995; Kluge and Nussbaum 1995; Daza 2008; Evans 2008). According to current phylogenetic hypotheses, this character must have evolved at least twice in the Gekkota, once in the sphaerodactylid *Pristurus* and the other in the Gekkonidae (Gamble *et al.* 2008b).

In conclusion, osteological data for *Narudasia* does little to resolve the phylogenetic uncertainty that has plagued the genus since its description nearly a century ago. However, it is evident that at least some its features are the result of miniaturization, whereas others may be reflective of at least distant affinities with some of the other Afro-Malagasy gekkonid genera, most notably *Rhoptropus* and *Ptenopus*. This ambiguity should not be surprising as it is also reflected in the very long branch and poorly supported nodes that subtend *Narudasia* in molecular phylogenetic analyses of all gekkotans (Gamble *et al.* 2008a,b; Bauer *et al.* unpublished data). However, it is likely that osteological data may prove more informative in the future. At present, osteological descriptions of this level of detail are only

available for a few scattered gekkotan taxa including *Coleonyx variegatus* (Kluge 1962) and *Sphaerodactylus roosevelti* (Daza *et al.* 2008) and even more superficial treatments only provide data for representatives of perhaps one half of all genera and <10% of all species (see Daza 2008 and Evans 2008; and references therein). As more complete comparative data sets become available and taxon complete morphologically based analyses become feasible, we expect that a more pronounced phylogenetic signal will emerge. Such evidence may be particularly important in cases like that of *Narudasia* in which even multilocus genetic analyses fail to resolve relationships and hard polytomies are implied (Dyke and van Tuinen 2004; Conrad *et al.* 2010).

Acknowledgements

References

Al Hassawi, A. M. 2007. *A Comparative Anatomy of the Neck Region in Lizards*, Trafford Publishing, Victoria, Canada.

Alexander, G. and Marais, J. 2007. *A Guide to the Reptiles of Southern Africa*. Struik, Cape Town.

Arnold, E. N. 1990. The two species of Moroccan day geckoes, *Quedenfeldtia* (Reptilia: Gekkonidae). – *Journal of Natural History*. **24**: 757–762.

Arnold, E. N. 1993. Historical changes in the ecology and behaviour of semaphore geckos (*Pristurus*, Gekkonidae) and their relatives. – *Journal of Zoology (London)*. **229**: 353–384.

Baird, I. L. 1960. A survey of the periotic labyrinth in some representative recent reptiles. – *The University of Kansas Science Bulletin* **41**: 891–981.

Baird, I. L. 1970. The anatomy of the reptilian ear. In Gans, C. and Parsons, T. S. (Eds): *Biology of the Reptilia, vol 2, Morphology B*. pp. 193–275, Academic Press, London and New York.

Bauer, A. M. 1986. *Systematics, biogeography and evolutionary morphology of the Carphodactylini (Reptilia: Gekkonidae)*. (PhD dissertation). University of California, Berkeley.

Bauer, A. M. 1989. Extracranial endolymphatic sacs in *Eurydactylodes* (Reptilia: Gekkonidae), with comments on endolymphatic function in lizards in general. – *Journal of Herpetology* **23**: 172–175.

Bauer, A. M. 1990a. Phylogeny and biogeography of the geckos of southern Africa and the islands of the western Indian Ocean: A preliminary analysis. In Peters, G. and Hutterer, R. (Eds): *Vertebrates in the Tropics: Proceedings of the International Symposium on Vertebrate Biogeography and Systematics in the Tropics, June 5–8, 1989*. pp. 274–284, Zologisches Forschungsinstitut und Museum A. Koenig, Bonn.

Bauer, A. M. 1990b. Phylogenetic systematics and biogeography of the Carphodactylini (Reptilia: Gekkonidae). – *Bonner zoologische Monographien* **30**: 1–217.

Bauer, A. M. 1999. Field guide to snakes and other reptiles of southern Africa (review). – *Copeia* **1999**: 236–238.

Bauer, A. M. 2010. A new species of *Pachydactylus* (Squamata: Gekkonidae) from the Otavi Highlands of northern Namibia. – *Bonn Zoological Bulletin* **57**: 257–266.

Bauer, A. M. and Branch, W. R. 2003 ("2001"). The herpetofauna of the Richtersveld National Park, Northern Cape Province, Republic of South Africa. – *Herpetological Natural History* **8**: 111–160.

Bauer, A. M. and Lamb, T. 2005. Phylogenetic relationships of southern African geckos in the *Pachydactylus* Group (Squamata: Gekkonidae). – *African Journal of Herpetology* **54**: 105–129.

Bauer, A. M., Barts, M. and Hulbert, F. 2006. A new species of the *Pachydactylus weberi* group (Reptilia: Squamata: Gekkonidae) from the Orange River, with comments on its natural history. – *Salamandra* **42**: 83–92.

Bell, C. J., Evans, S. E. and Maisano, J. A. 2003. The skull of the gymnophthalmid lizard *Neusticurus ecpleopus* (Reptilia: Squamata). – *Zoological Journal of the Linnean Society* **103**: 283–304.

Bever, G. S., Bell, C. J. and Maisano, J. A. 2005. The ossified braincase and cephalic osteoderms of *Shinisaurus crocodilurus* (Squamata, Shinisauridae). – *Palaentologia Electronica* **8**: 1–36.

Branch, W. R. 1988. *Field Guide to the Snakes and Other Reptiles of Southern Africa*. Struik, Cape Town.

Branch, W. R. 1993. *Southern African Snakes and Other Reptiles, A Photographic Guide*. Struik, Cape Town.

Branch, W. R. 1998. *Field Guide to the Snakes and Other Reptiles of Southern Africa*, 3rd edn. Struik, Cape Town.

de Burlet, H. M. 1934. Vergleichende Anatomie des stato–akustischen Organs. In Bolk, L., Göppert, E., Kallius, E. and Lubosch, W. (Eds): *Handbuch der Vergleichenden Anatomie der Wirbeltiere, Zweiter Band, 2. Hälfte*. pp. 1293–1432, Urban and Schwarzenberg, Berlin.

Conrad, J. L. 2004. Skull, mandible, and hyoid of *Shinisaurus crocodilurus* Ahl (Squamata: Anguimorpha). – *Zoological Journal of the Linnean Society* **141**: 399–434.

Conrad, J. L. and Norell, M. A. 2006. High-resolution X-ray computed tomography of an Early Cretaceous gekkonomorph (Squamata) from Öösh (Övörkhangai; Mongolia). – *Historical Biology* **18**: 405–431.

Conrad, J. L. and Norell, M. 2008. The braincase of two glyptosaurines (Anguidae, Squamata) and anguid phylogeny. – *American Museum Novitates* **3613**: 1–24.

Conrad, J. L., Ast, J. C., Montanari, S. and Norell, M. A. 2010. A combined evidence phylogenetic analysis of Anguimorpha (Reptilia: Squamata). – *Cladistics* **26**: 1–48.

Cope, E. D. 1900. The crocodilians, lizards, and snakes of North America. – *United States National Museum Annual Report* **1898**: 155–1294.

Daza, J. D. 2008. *Cladistic analysis of the Gekkota (Reptilia) by means of craniological data*. (PhD dissertation). University of Puerto Rico, San Juan.

Daza, J. D. and Bauer, A. M. 2010. The circumorbital bones of the Gekkota (Reptilia: Squamata). – *Anatomical Record* **293**: 402–413.

Daza, J. D., Abdala, V., Thomas, R. and Bauer, A. M. 2008. Skull anatomy of the miniaturized gecko *Sphaerodactylus roosevelti* (Squamata: Gekkota). – *Journal of Morphology* **269**: 1340–1364.

Daza, J. D., Herrera, A., Thomas, R. and Claudio, H. J. 2009. Are you what you eat? A geometric morphometric analysis of gekkotan skull shape. – *Biological Journal of the Linnean Society* **97**: 677–707.

Dyke, G. J. and van Tuinen, M. 2004. The evolutionary radiation of modern birds (Neornithes): Reconciling molecules, morphology and the fossil record. – *Zoological Journal of the Linnean Society* **141**: 153–177.

Estes, R., de Queiroz, K. and Gauthier, J. 1988. Phylogenetic relationships within Squamata. In Estes, R. and Pregill, G. K. (Eds): *Phylogenetic Relationships of The Lizard Families. Essays Commemorating Charles L Camp*. pp. 119–281, Stanford University Press, Stanford.

Evans, S. E. 2008. The skull of lizards and tuatara. In Gans, C., Gaunt, A. S. and Adler, K. (Eds): *Biology of the Reptilia, Vol 20, Morphology H: The skull of Lepidosauria*. pp. 1–347, Society for the Study of Amphibians and Reptiles, Ithaca.

Evans, S. E. and Manabe, M. 2008. An early herbivorous lizard from the Lower Cretaceous of Japan. – *Palaeontology* **51**: 487–498.

Feng, J., Han, D., Bauer, A. M. and Zhou, K. 2007. Interrelationships among gekkonid geckos inferred from mitochondrial and nuclear gene sequences. – *Zoological Science (Tokyo)* **24**: 656–665.

FitzSimons, V. F. 1938. Transvaal Museum expedition to South–West Africa and Little Namaqualand, May to August 1937. Reptiles and amphibians. – *Annals of the Transvaal Museum* **19**: 153–209, 1 map, pls. II–VI.

FitzSimons, V. F. 1943. The lizards of South Africa. – *Memoirs of the Transvaal Museum* **1**: XV + 528 pp., pls. I–XXIV, 1 folding map.

Frazzetta, T. H. 1962. A functional consideration of cranial kinesis in lizards. – *Journal of Morphology* **111**: 287–319.

Freeman, D. M. 1990. Anatomical model of the cochlea of the alligator lizard. – *Hearing Research* **49**: 29–37.

Gamble, T., Bauer, A. M., Greenbaum, E. and Jackman, T. R. 2008a. Out of the blue: A novel, trans–Atlantic clade of geckos (Gekkota, Squamata). – *Zoologica Scripta* **37**: 355–366.

Gamble, T., Bauer, A. M., Greenbaum, E. and Jackman, T. R. 2008b. Evidence for Gondwanan vicariance in an ancient clade of gecko lizards. – *Journal of Biogeography* **35**: 88–104.

Gamble, T., Bauer, A. M., Colli, G. R., Greenbaum, E., Jackman, T. R., Vitt, L. J. and Simons, A. M. 2011. Coming to America: Multiple origins of New World geckos. – *Journal of Evolutionary Biology* **24**: 231–244.

Ganeshina, O. and Vorobyev, M. 2003. Contractile cochlear frame in the gecko *Teratoscincus scincus*. – *The Journal of Comparative Neurology* **461**: 539–547.

Ganeshina, O. and Vorobyev, M. 2009. A contractile cochlear frame is a common feature of the hearing organs in Gekkota (Sauria, Squamata): A comparative study. – *Brain, Behavior and Evolution* **74**: 87–101.

Gardiner, B. G. 1982. Tetrapod classification. – *Zoological Journal of the Linnean Society* **74**: 207–232.

Griffin, M. 1998. Reptile diversity. In Barnard, P. (Ed): *Biological Diversity in Namibia: A Country Study*. pp. 148–154, Namibian National Biodiversity Task Force, Windhoek.

Griffin, M. 2000. Annotated checklist of amphibians, reptiles and mammals of the Brandberg, central Namib Desert, Namibia. – *Cimbebasia Memoirs* **9**: 69–89.

Griffin, M. 2002. *Annotated Checklist and Provisional National Conservation Status of Namibian Reptiles*. Directorate of Scientific Services, Ministry of the Environment and Tourism, Windhoek. 171 pp.

Griffin, M. 2003. *Annotated Checklist and Provisional National Conservation Status of Namibian Reptiles*. Namibia Scientific Society, Windhoek. 169 pp.

Gugg, W. 1939. Der Skleralring der plagiotremen reptilien. – *Zoologische Jahrbücher, Abteilung für Anatomie und Ontogenie der Tiere* **65**: 339–416.

Haacke, W. D. 1970. New herpetological records from south West Africa. – *Annals of the Transvaal Museum* **26**: 277–283.

Haacke, W. D. 1976. The burrowing geckos of southern Africa. 5 (Reptilia: Gekkonidae). – *Annals of the Transvaal Museum* **30**: 71–89.

Haacke, W. D. 1997. Family Gekkonidae. Genus *Pachydactylus* and other western arid area representatives. In Van Wyk, J. H. (Ed): *Proceedings of the FitzSimons Commemorative Symposium. South African Lizards: 50 Years of Progress and Third H.A.A. Symposium on African Herpetology*. pp. 40–43, The Herpetological Association of Africa, Stellenbosch.

Hall, B. K. 2005. *Bones and Cartilage. Developmental and Evolutionary Skeletal Biology*. Elsevier, Academic Press, San Diego.

Hamilton, D. W. 1960. Observations on the morphology of the inner ear in certain gekkonoid lizards. – *The University of Kansas Science Bulletin* **41**: 983–1024.

Hamilton, D. W. 1964. The inner ear of lizards. I. Gross structure. – *Journal of Morphology* **115**: 255–272.

Han, D., Zhou, K. and Bauer, A. M. 2004. Phylogenetic relationships among gekkotan lizards inferred from C–mos nuclear DNA sequences and a new classification of the Gekkota. – *Biological Journal of the Linnean Society* **83**: 353–368.

Häupl, M. 1980. Das Schädelskelett einiger Arten der Fam. Gekkonidae. – *Annalen des Naturhistorischen Museums in Wien* **83**: 479–518.

Hedges, S. B. and Thomas, R. 2001. At the lower size limit in amniote vertebrates: A new diminutive lizard from the West Indies. – *Caribbean Journal of Science* **37**: 168–173.

Holder, L. A. 1960. The comparative morphology of the axial skeleton in the Australian Gekkonidae. – *Journal of the Linnean Society of London Zoology* **44**: 300–335.

Iordansky, N. 1966. Cranial kinesis in lizards: Contribution to the problem of the adaptive significance of skull kinesis [in Russian]. – *Zoologicheskii Zhurnal* **45**: 1398–1410.

Jerez, A., Mangione, S. and Abdala, V. 2010. Occurrence and distribution of sesamoid bones in squamates: A comparative approach. – *Acta Zoologica* **91**: 295–305.

Johnston, P. 2010. The constrictor dorsalis musculature and basipterygoid articulation in *Sphenodon*. – *Journal of Morphology* **271**: 280–292.

Jollie, M. T. 1960. The head skeleton of the lizard. – *Acta Zoologica (Stockholm)* **41**: 1–54.

Kluge, A. G. 1962. Comparative osteology of the eublepharid genus *Coleonyx* Gray. – *Journal of Morphology* **110**: 299–332.

Kluge, A. G. 1967. Higher taxonomic categories of gekkonid lizards and their evolution. – *Bulletin of the American Museum of Natural History* **135**: 1–60.

Kluge, A. G. 1976. Phylogenetic relationships in the lizard family Pygopodidae: An evaluation of theory, methods and data. – *Miscellaneous Publications of the Museum of Zoology, University of Michigan* **152**: 1–72.

Kluge, A. G. 1982. Cloacal bones and sacs as evidence of gekkonoid lizard relationships. – *Herpetologica* **38**: 348–355.

Kluge, A. G. 1987. Cladistic relationship in the Gekkonoidea (Squamata, Sauria). – *Miscellaneous Publications of the Museum of Zoology, University of Michigan* **173**: 1–54.

Kluge, A. G. 1995. Cladistic relationships of sphaerodactyl lizards. – *American Museum Novitates* **3139**: 1–23.

Kluge, A. G. and Nussbaum, R. A. 1995. A review of African–Madagascan Gekkonid lizard phylogeny and biogeography (Squamata).

– *Miscellaneous Publications of the Museum of Zoology, University of Michigan* **183**: 1–20.

Kuhn, G., Gruber, P., Müller, R. and Rühli, F. 2008. Three–dimensional evaluation of structures in small bones by Micro–CT: Tail fracture planes of autotomizing lizards (Scincidae and Gecconidae [sic] families). – *The Internet Journal of Biological Anthropology* **1**: 1.

Lakjer, T. 1927. Studien über die Gaumenregion bei Sauriern im Vergleich mit Anamniern und primitiven Sauropsiden. – *Zoologische Jahrbücher, Abteilung für Anatomie und Ontogenie der Tiere* **38**: 57–356.

Lawrence, R. F. 1936. The prostigmatic mites of South African lizards. – *Parasitology* **27**: 1–45.

Loveridge, A. 1947. Revision of the African lizards of the family Gekkonidae. – *Bulletin of the Museum of Comparative Zoology* **98**: 1–469, pls. 1–7, 1 folding table.

McDowell, S. B. 1967. The extracolumella and tympanic cavity of the ''earless'' monitor lizard, *Lanthanotus borneensis*. – *Copeia* **1967**: 154–159.

Mertens, R. 1955. Die Amphibien und Reptilien Südwestafrikas aus den Ergebnissen einer im Jahre 1952 ausgeführten Reise. – *Abhandlungen der Senckenbergischen Naturforschenden Gesellschaft* **490**: 1–172.

Mertens, R. 1971. Die Herpetofauna Südwest-Afrikas. – *Abhandlungen der Senckenbergischen Naturforschenden Gesellschaft* **529**: 1–110.

Methuen, P. A. and Hewitt, J. 1914. The percy sladen memorial expedition to great namaqualand 1912–1913. Records and descriptions of the reptiles and batrachians of the collection. – *Annals of the Transvaal Museum* **4**: 118–145.

Miller, M. R. 1966. The cochlear duct of lizards and snakes. – *American Zoologist* **6**: 421–429.

Moffat, L. A. 1973. The concept of primitiveness and its bearing on the phylogenetic classification of the Gekkota. – *Proceedings of the Linnean Society New South Wales* **97**: 275–301.

Noble, G. K. 1921. The bony structure and phyletic relations of *Sphaerodactylus* and allied lacertilian genera, with the description of a new genus. – *American Museum Novitates* **4**: 1–16.

Oelrich, T. M. 1956. The anatomy of the head of *Ctenosaura pectinata* (Iguanidae). – *Miscellaneous Publications of the Museum of Zoology, University of Michigan* **94**: 1–122.

Olori, J. C. 2010. Digital endocasts of the cranial cavity and osseous labyrinth of the burrowing Snake *Uropeltis woodmasoni* (Alethinophidia: Uropeltidae). – *Copeia* **2010**: 14–26.

Parker, H. W. 1936. Dr. Karl Jordan's Expedition to South–West Africa and Angola: Herpetological collections. – *Novitates Zoologicae* **40**: 115–146.

Payne, S. L., Holliday, C. M. and Vickaryous, M. K. 2011. An osteological and histological investigation of cranial joints in geckos. – *Anatomical Record* **294**: 399–405.

Rieppel, O. 1984a. The structure of the skull and jaw adductor musculature of the Gekkota, with comments on the phylogenetic relationships of the Xantusiidae (Reptilia: Lacertilia). – *Zoological Journal of the Linnean Society* **82**: 291–318.

Rieppel, O. 1984b. Miniaturization of the lizard skull: Its functional and evolutionary implications. In Ferguson, M. W. J. (Ed): *The Structure, Development and Evolution of Reptiles (Zoological Symposium No. 52)*. pp. 503–520, The Zoological Society of London, Academic Press, London.

Rieppel, O. 1985. The recessus scalae tympani and its bearing on the classification of reptiles. – *Journal of Herpetology* **19**: 373–384.

Rieppel, O. 1996. Miniaturization in tetrapods: Consequences for skull morphology. In Miller, P. J. (Ed): *Miniature Vertebrates: The Implications of Small Body Size (Zoological Symposium No. 69)*. pp. 15–45, Clarendon Press, Oxford.

Rieppel, O., Gauthier, J. and Maisano, J. A. 2008. Comparative morphology of the dermal palate in squamate reptiles, with comments of phylogenetic implications. – *Zoological Journal of the Linnean Society* **152**: 131–152.

Röll, B. 2001. Multiple origin of diurnality in geckos: Evidence from eye lens crystallins. – *Naturwissenschaften* **88**: 293–296.

Romer, A. S. 1956. *Osteology of the Reptiles*. University of Chicago Press, Chicago.

Russell, D. A. 1967. Systematics and morphology of American mosasaurs. – *Bulletin of the Peabody Museum of Natural History* **23**: 1–241.

Russell, A. P. 1972. *The foot of gekkonid lizads: A study in comparative and functional anatomy*. PhD dissertation. University of London, London.

Russell, A. P. and Bauer, A. M. 2002. Underwood's classification of geckos: A 21st century appreciation. – *Bulletin of the Natural History Museum, London, Zoology series* **68**: 113–121.

Russell, A. P. and Bauer, A. M. 2008. The appendicular locomotor apparatus of, and locomotion in lizards and *Sphenodon*. In Gans, C., Gaunt, A. S. and Adler, K. (Eds): *Biology of the Reptilia, Vol 21, Morphology I: The Skull and Appendicular Locomotor Apparatus of Lepidosauria*. pp. 1–466, Society for the Study of Amphibians and Reptiles, Ithaca.

Shute, C. C. D. and Bellairs, A. d'. A. 1953. The cochlear apparatus of Geckonidae and Pygopodidae and its bearing on the affinities of these groups of lizards. – *Proceedings of the Zoological Society of London* **123**: 695–708.

Stephenson, N. G. and Stephenson, E. M. 1956. The osteology of the New Zealand geckos and its bearing in their morphological status. – *Transactions of the Royal Society of New Zealand* **84**: 341–358.

Stuart, C. T. 1980. And annotated preliminary list of amphibians and reptiles known to occur in the Namib Desert Park, Namibia. – *Journal of the Herpetological Association of Africa* **24**: 4–13.

Underwood, G. 1954. On the classification and evolution of geckos. – *Proceedings of the Zoological Society of London* **124**: 469–492.

Underwood, G. 1957. On lizards of the family Pygopodidae. A contribution to the morphology and phylogeny of the Squamata. – *Journal of Morphology.* **100**: 207–268.

Underwood, G. 1970. The eye. In Gans, C. and Parsons, T. S. (Eds): *Biology of the Reptilia, Vol 2, Morphology B.* pp. 1–97, Academic Press, London and NewYork.

Versluys, J. 1912. Das Streptostylie Problem und die Bewegungen im Schädel bei Sauropsiden. – *Zoologische Jahrbücher, Abteilung für Anatomie und Ontogenie der Tiere* **15**: 545–714.

Visser, J. 1984. Feesgeitjie, fluweelgeitjie en huisgeitjie. – *Landbouweekblad* **20**: 64–65.

Wiedersheim, R. 1875. Zur Anatomie und Physiologie des *Phyllodactylus europaeus*, mit besonderer Berücksichtigung des Aquaeductus vestibuli der Ascalaboten im Allgemeinen. Zugleich als zweiter Beitrag zur Inselfauna des Mittelmeeres. – *Morphologiches Jahrbuch* **1**: 495–534, pls. XVII–XIX.

Wyeth, F. J. 1924. The development of the auditory apparatus in *Sphenodon punctatus* with an account of the visceral pouches, aortic arches, and other accesory structures. – *Philosophical Transactions of the Royal Society B* **212**: 259–368.

Appendix – Vouchered Localities for *Narudasia festiva*

Locality data have been taken from collection records (see Materials and Methods for museum acronyms). Latitude and

longitude are generally given only when the collectors determined this themselves using a GPS or topographic map, or when georeferenced by the relevant museum. Regardless of the original form in which coordinates were recorded, we have presented them here in the form of degrees, minutes, seconds. For localities without precise coordinates, we have determined quarter degree square references (QDS). The QDS system has been nearly universally used in large-scale mapping of the southern African biota and remains a convenient approach to dealing with distributions. Under this system of notation, each single degree square is subdivided into four quarter degrees, designated A–D (A = NW quadrant, B = NE quadrant, C = SW quadrant, D = SE quadrant). Each quarter degree is in turn divided into four similarly designated divisions, yielding a basic unit one sixteenth of a degree square, or one quarter of a degree on a side (e.g. 3015Ac represents the unit bounded by 30°15′S and 30°30′S and 15°00′E and 15°15′E). All QDS references are to degrees South and East. We have corrected some QDS references that were clearly incorrect. All localities have been grouped by Region, then District within Namibia and by QDS within each district.

Namibia: OTJOZONDJUPA REGION, Okahandja District: CAS 85932, 15 mi. northwest of Okahandja (2116Dd); SMF 65921–22, 10 mi E Okahandja (2117Cc); ERONGO REGION, Swakopmund District: TM 44342–44, Mirabib Hills, Namib Naukluft Park (2214Da); SMF 21668, Goanikontes, Swakoptal, (22°40′S, 14°50′E); TM 56645-56647, Palmenhorst, (22°41′S, 14°53′E); NMN 4159, 1 km N. of Roessing Rio Tinto Mine (22°23′S, 15°05′E); NMN 4261, Upper Panner Gorge test site, Roessing (22°28′S, 15°00′E); NMN 5391, 4 km E of Arandis Mtn. (22°23′S, 15°03′E); NMN 5392, 2 km. N of Roessing Mine, (22°26′S, 15° 02′E); NMN 4157, Roessing Stock Pile (22°28′S, 15°02′E); SAM ZR 46937, Swakop River, 60 km up (2215Ca); TM 32599–600, Langer Heinrichberg (22°48′S, 15°20′E); SAM ZR 46531 N of Gobabeb, (2315Aa); TM 48775, 20 km. from Namib Naukluft Park Gate (2215Ac); TM 31345, Hills 4.8 km. NNW of Gorob Mine, Namib Naukluft Park, (23°29′S, 15°24′E); TM 47129, 48230, 48242–43, 48246, 48261, Farm Changans, (23°04′S, 15°55′E); NMN 3269, Homeb Canyon above Hottentot village, Namib Desert Park (2315Ca); TM 47125, Gobabeb (23°34′S, 15°03′E); MCZ Z23252-68 (in AMB collection), Homeb (2315Ca); TM 25929, 28401, Namib Naukluft National Park (23°33′S, 15°17′E); AMG 99, CAS 121148, PEM R14676, Gorob (2315Cb); AMG 101, 3 mi from turn off to Zebra Pan, 45 mi E Gobabeb (2315Cb); AMG 100, PEM R14673–74, Turn-off to Zebra Pan, 45 mi East of Gobabeb, (2315Cb); AMB 8945, 8957–58, 896, Zebra Pan (2315 Da); PEM R11335, Hope Mine, Namib Desert Park (2315Cb); SMF 51789, Farm Tjab [=Djab], SW Windhoek (23°15′S, 16°05′E); KHOMAS REGION, Windhoek District: SAM ZR 46640, Auanis (306) (2216Ca); TM 41959, 41968, Farm Aub (22°42′S, 16°30′E); TM 57870, Farm Uruganus (358) (22°51′S 16°17′E); NMN 1923, Keres (89)

(2216Db); NMN 7868, Otjompaue (40) (2216Db); NMN 83, TM 17490, 17492, 17507, 17509-10, Farm Neudamm (63) (22°26′S, 17°20′E); ZFMK 18360, Frauenstein, N/a'an ku se Lodge and Wildlife Sanctuary (22°21′52.52″S, 17°22′44.87″E); BMNH 1988.427–428, Regenstein Mt., ca. 16 km. S. Windhoek (22°43′59″S, 17°02′06″E); CAS 167650, NMN 86, Windhoek (2217Ca); ZFMK 18359, Windhoek (22°33′32.05″S, 17°04′56.94″E); CAS 167651, Moltkeblick Mtn., 2446 m (22°39′S, 17°11′E); NMN 5375–84, Moltkeblick, Auas Mtns. (22°39′S, 17°10′E); NMN 88, Goreangab Dam, Windhoek (2217Ca); TM 63523, Farm Protea (108) (22°46′S, 17°45′E); TM 26026, Farm Schlesien (2315Bb); TM 56610–11, Farm Chausib (23°20′S, 16°05′E); HARDAP REGION, Rehoboth District: PEM R2159, 2164, Borodino Ranch (2316Cb); SAM ZR 46931, Nauchas (2316Cb); TM 48438–40, Farm Nauchas (14) (23°39′S, 16°18′E); CAS 223902, 5.0 km SW Kobos, 1590 m, (23°37′20″S, 16°41′36″E); NMN 85, PEM R2158, Kobos (321) (2316 Da); TM 44164–66, Gaub River Bridge, Farm Greylingshof near Rehoboth (2317Ac); CAS 206932, Oanab Dam campsite, 7 km NW Rehoboth (2317Ac); SAM ZR 46928, Rietoog (2416Ba); Maltahöhe District: SAM ZR 45523, Zaris Pass (2416Cd); Mariental District: BMNH 1936.8.1.369, Satansplatz (24°52′S, 17°33′E); KARAS REGION, Bethanie District: MCZ R188255, 3 km. N. Farm Barby House on C27 (25°50′54.2″S, 16°31′39.0″E); MCZ A-27027 (to be accessiond in NMN), Farm Barby (25°50′08.8″S, 16°32′08.6″E); CAS 106031, FMNH 218640, MCZ R46801-02, PEM R2163, SAM ZR 46495, NMN 84, Farm Barby, 20 mi. W. of Helmeringshausen (2516Dc); TM 17588, 17590, 17393, 17610, 17612, 17615–19, 17644, 17683–17686, Farm Barby, (25°50′S, 16°35′E); NMN 87, Tiras (33) (2616Ba); TM 28419, Farm Tiras, (26°10′S, 16°36′E); MCZ R184348, Helmeringhausen-Aus Rd. (C13) (26°04′48.01″S, 16°38′24.02″E); SAM ZR 46482, Naiams (83), 17 km. W. of Seeheim (2617 Da); Keetmanshoop District: SAM ZR 46483, Gurieb River, Sandverhaar (2517Cd); MCZ R185988, Brukkaros Mountain (25°53′49″S, 17°46′38″E); TM 17790–91, 17797–98, 41817–18, Brukkaros Mountain (25°52′, 17°47′); USNM 84940.60584, 84941.60584, Mt. Brukkaros (2517Dd); Karasburg District: BMNH 1946.8.20.47, TM 3031–33, 3036–38, 3042, 3044–48, Rocky river bed, Narudas Süd, Farm Narudas (268) at foot of east side Gt. Karas Mts. (27°21′S, 18°51′E); CAS 186278, Farm Garub, 2 km. S of turnoff to Narudas (2718Bd); CAS 186288–91, AMB 3239, 3241, 3243, Farm Narudas Süd at river (2718Bd); CAS 186296–99, AMB 3250, 3253–54, 3256, Farm Narudas Süd, 0.5 km N of house (2718Bd); CAS 223894–95, Farm Narudas, ca 0.3 km N. of house (27°22′11″S, 18°51′28″E); MCZ R186004–05, Farm Narudas, (27°22′12″S, 18°51′29″E); MCZ R186006–07, Farm Narudas, at river crossing (27°23′22″S, 18°52′23″E); MCZ R14209, R41818, Narudas Süd (2718Bd); CAS 201871, 203510, 223894, AMB 4963, 4365, Ai-Ais Nature Reserve, ca 3 km. from Orange River

(28°12′26″S, 17°16′43″E); LÜDERITZ DISTRICT: TM 48352, Farm Plateau (26°37′S, 16°29′E); PEM R2160–62, Pockenbank (2716Ba); SAM ZR 43641–42, 43645, Namuskluft Inselberg (2716Dd); SAM ZR 43651–53, Zebrafontein (2716Dd); NMN 167, 2702, Namuskluft (88) (2716Dd); TM 35333, 35364–66, Farm Namuskluft (27°56′S, 16°54′E); TM 35401–03, 35462, Macmillans Pass top, 11 mi NE of Rosh Pinah (27°56′S, 16°54′E); PEM R12533, 7.6 km. Northwest of Fish River Mouth (2817Aa); AMB 4976–77, 7.6 km. W of Fish River Mouth (28°03′45″S, 17°07′25″E); PEM R12529, 77 km from Noordower, Ais-Ais Reserve (28°12′26″S, 17°16′43″E). NO PRECISE LOCALITY: AMG 98, PEM R14675, YPM HERR.015940. QUESTIONABLE LOCALITY: *South Africa*: NORTHERN CAPE PROVINCE: CAS 167652, just S of Orange River (this locality is almost certainly in error and the likely correct locality is just N of Orange River, probably in the vicinity of the Fish River Mouth),